Host Protein BSL1 Associates with *Phytophthora infestans* RXLR Effector AVR2 and the *Solanum demissum* Immune Receptor R2 to Mediate Disease Resistance[C][W]

Diane G.O. Saunders,[a] Susan Breen,[b,c] Joe Win,[a] Sebastian Schornack,[a] Ingo Hein,[b] Tolga O. Bozkurt,[a] Nicolas Champouret,[a] Vivianne G.A.A. Vleeshouwers,[d] Paul R.J. Birch,[b,c,1] Eleanor M. Gilroy,[b] and Sophien Kamoun[a,1,2]

[a] The Sainsbury Laboratory, Norwich Research Park, Norwich NR4 7UH, United Kingdom
[b] Cell and Molecular Sciences, James Hutton Institute, Invergowrie, Dundee DD2 5DA, United Kingdom
[c] Division of Plant Sciences, University of Dundee (at James Hutton Institute), Invergowrie, Dundee DD2 5DA, United Kingdom
[d] Wageningen UR Plant Breeding, 6700 AJ Wageningen, The Netherlands

Plant pathogens secrete effector proteins to modulate plant immunity and promote host colonization. Plant nucleotide binding leucine-rich repeat (NB-LRR) immunoreceptors recognize specific pathogen effectors directly or indirectly. Little is known about how NB-LRR proteins recognize effectors of filamentous plant pathogens, such as *Phytophthora infestans*. AVR2 belongs to a family of 13 sequence-divergent *P. infestans* RXLR effectors that are differentially recognized by members of the R2 NB-LRR family in *Solanum demissum*. We report that the putative plant phosphatase BSU-LIKE PROTEIN1 (BSL1) is required for R2-mediated perception of AVR2 and resistance to *P. infestans*. AVR2 associates with BSL1 and mediates the interaction of BSL1 with R2 in planta, possibly through the formation of a ternary complex. Strains of *P. infestans* that are virulent on R2 potatoes express an unrecognized form, *Avr2-like* (referred to as *A2l*). A2L can still interact with BSL1 but does not promote the association of BSL1 with R2. Our findings show that recognition of the *P. infestans* AVR2 effector by the NB-LRR protein R2 requires the putative phosphatase BSL1. This reveals that, similar to effectors of phytopathogenic bacteria, recognition of filamentous pathogen effectors can be mediated via a host protein that interacts with both the effector and the NB-LRR immunoreceptor.

INTRODUCTION

A central question in plant pathology is how pathogens are recognized by their hosts and how the subsequent activation of immunity may be evaded or suppressed by pathogens to promote disease. Plants recognize pathogens and mount active defenses to attenuate pathogen progression. First, plant basal defense responses are activated by the perception of pathogen-associated molecular patterns by pattern recognition receptors at the plant cell surface, resulting in pathogen-associated molecular pattern–triggered immunity (Jones and Dangl, 2006). However, pathogens secrete an array of proteins, known as effectors, to suppress these basal defense mechanisms. A second wave of defense acts largely within the cell through the genetically determined recognition of a subset of pathogen effectors, known as avirulence (AVR) proteins. This immune response is mediated by a sophisticated surveillance mechanism that consists of highly specific and structurally conserved plant disease resistance (R) proteins (Jones and Dangl, 2006; van der Hoorn and Kamoun, 2008; Elmore et al., 2011). Each R protein recognizes one or a few corresponding AVR effectors, leading to the activation of effector-triggered immunity (ETI) that often results in a rapid, localized host cell death, termed the hypersensitive response (HR). However, pathogens can also secrete effectors to suppress ETI and promote disease progression (Jones and Dangl, 2006). The fundamental questions in this coevolutionary arms race remain: What are the host targets of effector proteins, why are these proteins targeted, and how do plants sense pathogen effectors? This is particularly relevant for oomycetes and fungi, the filamentous pathogens that cause the most destructive plant diseases. Little is known about the targets of filamentous pathogen effectors and the mechanisms by which these effectors modulate immunity.

Over the past two decades, significant numbers of *R* genes have been identified. The largest family functions as immune receptors and encode nucleotide binding leucine-rich repeat (NB-LRR) proteins that mediate recognition of pathogen-derived AVR effectors (Eitas and Dangl, 2010; Elmore et al., 2011). Recognition of AVR molecules can be either direct, through interaction with their cognate R proteins, or indirect, through the perception of modifications in host proteins targeted by the AVR effector (Chisholm et al., 2006; Jones and Dangl, 2006; van der Hoorn and Kamoun, 2008; Elmore et al., 2011). In filamentous pathogens, a few instances of direct interaction between an

NB-LRR immune receptor and an effector have been confirmed experimentally (Jia et al., 2000; Dodds et al., 2006; Krasileva et al., 2010). Among the oomycetes, one example is the recognition of *Hyaloperonospora arabidopsidis* ATR1 by *Arabidopsis thaliana* RPP1, where association of ATR1-RPP1 is dependent on interaction with the LRR domain of the NB-LRR immune receptor (Krasileva et al., 2010). More recently, evidence of direct interaction between *Phytophthora infestans* effector ipiO (AVRblb1) and the coiled-coil domain of RB (Rpi-blb1) has been reported (Chen et al., 2012). In bacterial systems, effectors are often recognized indirectly through the perception of modifications in an accessory host protein (Elmore et al., 2011). For instance, *Pseudomonas syringae* AVR proteins AvrB and AvrRpm1 are indirectly recognized by the *Arabidopsis* NB-LRR protein RPM1 that detects pathogen proteins that mediate phosphorylation of the host target protein RIN4 (Liu et al., 2011). Remarkably, so far, indirect recognition of fungal and oomycete AVR effectors by NB-LRR proteins has not been described even though several cases of direct recognition have been reported (Jia et al., 2000; Dodds et al., 2006; Krasileva et al., 2010).

The study of indirect recognition in well-characterized pathogen systems has led to the development of two models known as the guard and decoy hypotheses. In the guard model, the R protein monitors the status of a host protein, the guardee, which is also required for the virulence function of the effector in the absence of the R protein (van der Hoorn and Kamoun, 2008). By contrast, in the decoy model, the targeted protein acts mainly in effector recognition, mimicking the operative target to activate ETI (van der Hoorn and Kamoun, 2008). The extent to which these models apply to the perception of filamentous pathogen AVR effectors by NB-LRR receptors is unknown. A crucial step is to uncover the host targets of the ever-increasing list of characterized filamentous pathogen AVR effectors. So far, only limited numbers of host targets of these effectors have been described and none have been implicated in perception by NB-LRR proteins (Oliva et al., 2010).

Biotrophic fungi and oomycetes secrete effectors from highly specialized structures, known as haustoria, which form at pathogen-directed invaginations of the host plasma membrane (Panstruga and Dodds, 2009). Once secreted into the extrahaustorial matrix, some effectors translocate into the host cell where they modulate plant immunity (Stassen and Van den Ackerveken, 2011). In oomycetes, such as *Phytophthora* and downy mildews, the largest class of host-translocated effectors are the RXLR-type proteins, which include all known AVR effectors (Hein et al., 2009; Vleeshouwers et al., 2011). RXLR effectors have a modular architecture with the N-terminal signal peptide and RXLR domain involved in secretion and host translocation and the C-terminal domain carrying the biochemical effector activity (Win et al., 2007). Evolutionary analyses demonstrate that positive selection has acted mainly on the effector domain, probably as a consequence of coevolution with plant targets and/or resistance genes (Win et al., 2007). All *Phytophthora* genomes examined to date carry a large repertoire of RXLR effector genes. *P. infestans*, the agent of the economically important potato late blight disease, harbors ~550 RXLR effector genes, of which seven out of 127 families have been assigned an AVR activity (Haas et al., 2009; Vleeshouwers

et al., 2011). These effectors provide a wealth of molecular probes that can be used to unravel novel components of the immune system.

Among the *P. infestans* AVR effectors, the recently described AVR2 is a canonical RXLR effector protein of 116 amino acids that elicits HR in the presence of the wild potato (*Solanum demissum*) NB-LRR protein R2 (Gilroy et al., 2011). *R2* belongs to a highly diverse gene family located at a major late blight resistance locus on chromosome IV of potato (*Solanum tuberosum*; Lokossou et al., 2009; Vleeshouwers et al., 2011). Several *R2* alleles and orthologs from six different *Solanum* species have been shown to recognize AVR2 and confer resistance to *P. infestans* (Champouret, 2010). In *P. infestans* strain T30-4, *Avr2* belongs to a family of 18 genes encoding 13 sequence-divergent members that share similarity throughout the C-terminal effector domains and range from 94 to 118 amino acids (Haas et al., 2009; Champouret, 2010; Vleeshouwers et al., 2011). Several of the AVR2 homologs are specifically recognized inside plant cells by R2 (Champouret, 2010), although genetic analyses of a cross between a virulent and avirulent race has revealed one gene, *Avr2* (also known as *PITG_22870*), as the major contributor to the avirulence phenotype (van der Lee et al., 2001; Gilroy et al., 2011). Strains of *P. infestans* that are virulent on *R2* potatoes either do not express *Avr2* and/or express a distinct variant, *Avr2-like* (referred to here as *A2l* to avoid confusion with other homologs), that evades perception by R2 (Gilroy et al., 2011). The *A2l* form was initially isolated from the aggressive clonal lineage genotype 13_A2 (blue13) that has been responsible for destructive potato late blight epidemics in Great Britain since 2007 (Fry et al., 2008; Gilroy et al., 2011). The polymorphic nature of the *AVR2* and *R2* families, and the occurrence of the latter in Central Mexico, a center of *P. infestans* diversity, is indicative of coevolutionary balancing selection between *P. infestans* and *Solanum* hosts (Champouret, 2010; Vleeshouwers et al., 2011). This system provides a unique opportunity to study differential host recognition and evolution of virulence involving a filamentous pathogen family of host-translocated effectors.

In this study, we used a recently developed in planta coimmunoprecipitation (co-IP) protocol (Win et al., 2011) to identify host targets of AVR2. We discovered that AVR2 associates in planta with BSL1, a kelch repeat domain–containing putative phosphatase. The AVR2–BSL1 interaction was independently confirmed using yeast two-hybrid (Y2H) assays. Not all of the 13 AVR2 family members interacted with BSL1. Remarkably, the five AVR2 homologs that interacted with BSL1 are the only family members that are perceived by R2, pointing to a possible role of BSL1 in R2-mediated recognition. Virus-induced gene silencing (VIGS) experiments demonstrated that BSL1 is required for R2-mediated recognition of AVR2 and resistance to *P. infestans*. We also discovered that BSL1 associates with R2, but only in the presence of AVR2, possibly through the formation of a ternary complex. Interestingly, A2L, which evades recognition by R2, nevertheless interacts with BSL1. However, unlike AVR2, A2L did not promote the interaction of BSL1 with R2. Our findings show that recognition of the *P. infestans* AVR2 effector by the NB-LRR protein R2 requires the host protein BSL1. This reveals that, similar to effectors of phytopathogenic bacteria,

A
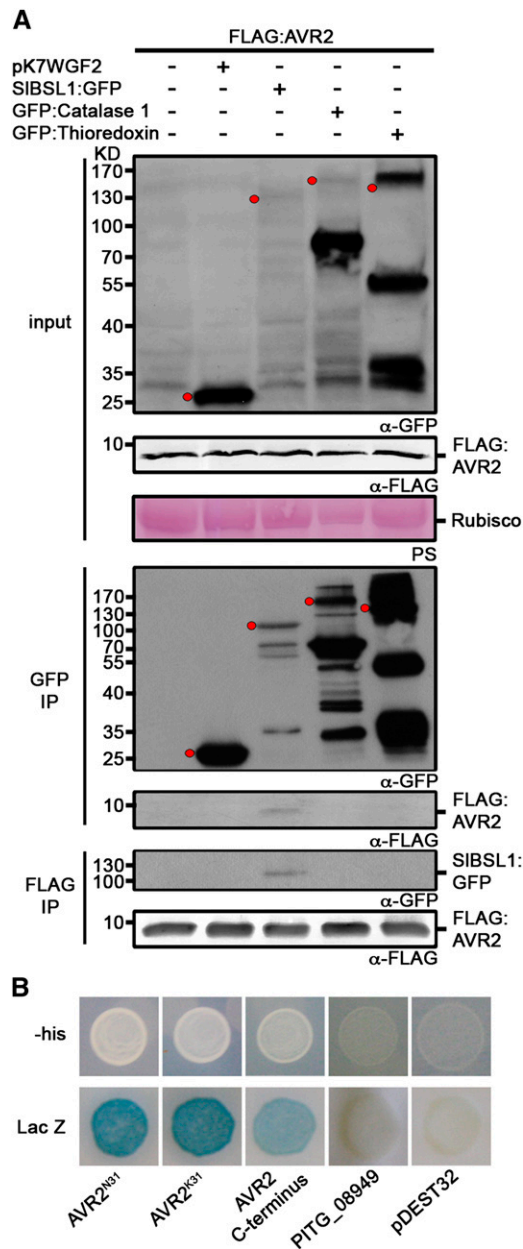
Figure 1. *P. infestans* AVR2 Specifically Associates with BSL1.

(A) Immunoblots showing AVR2 specifically coimmunoprecipitates with tomato BSL1 (Sl-BSL1) in planta. FLAG:AVR2 was transiently expressed alone, with the empty vector pK7WGF2 or with GFP-tagged putative target proteins in *N. benthamiana*. Immunoprecipitates (IP) obtained with anti-FLAG or anti-GFP antiserum and total protein extracts were immunoblotted with appropriate antisera. The expected sizes of the GFP fusion proteins are indicated by red dots in the crude extracts and GFP co-IP probed with anti-GFP antibody. PS, Ponceau stain; Rubisco, ribulose-1,5-bisphosphate carboxylase/oxygenase.

(B) Y2H analysis illustrating that the two allelic variants of AVR2, *P. infestans* $AVR2^{K31}$ and $AVR2^{N31}$, and the C-terminal effector domain of AVR2 (amino acids 66 to 116) interact with potato BSL1 (St-BSL1) in vivo. Both *LacZ* (blue) and *His3* (providing growth on medium lacking His [-his]) reporter genes were activated. Empty vector (pDEST32) was used

recognition of filamentous pathogen effectors can be mediated through a host protein that interacts with both the effector and the NB-LRR immunoreceptor (Elmore et al., 2011).
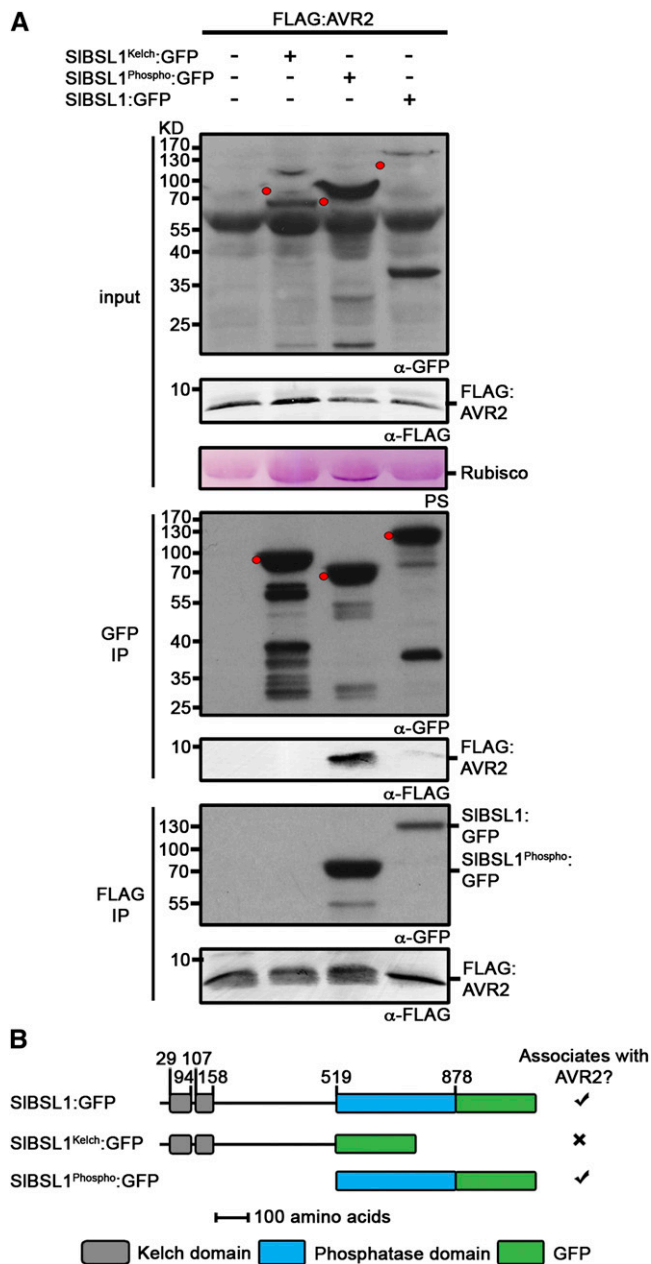
RESULTS

AVR2 Interacts with the Putative Phosphatase BSL1

To identify host targets of AVR2, we used in planta co-IP followed by liquid chromatography–tandem mass spectrometry (LC-MS/MS) (Win et al., 2011). The C-terminal effector domains of each of the 13 AVR2 family members were fused to the FLAG epitope tag at the N terminus in place of the signal peptide and RXLR domain (see Supplemental Figure 1A online). These constructs were expressed in *Nicotiana benthamiana* leaves using *Agrobacterium tumefaciens*–mediated transient transformation (agroinfiltration) before being used in co-IPs. Three plant proteins, peroxisomal enzyme catalase 1, thioredoxin peroxidase, and a phosphatase of the BSL family (BSU-LIKE PROTEIN1 [BSL1]), specifically associated with one or more of the eight AVR2 homologs that formed protein complexes detectable by LC-MS/MS (see Supplemental Table 1 and Supplemental Data Set 1 online). To confirm and further study the associations, the three putative target proteins were cloned and fused to green fluorescent protein (GFP). Using co-IPs, we validated the specific in planta association between AVR2 and tomato (*Solanum lycopersicum*) BSL1 (Sl-BSL1) but not the other two plant proteins (Figure 1A). To determine the extent to which these findings apply to other AVR2 homologs, we also examined PEXRD11, an RXLR effector that was previously shown to activate R2 (Champouret, 2010). PEXRD11 also specifically immunoprecipitated with Sl-BSL1 but not the other two plant proteins (see Supplemental Figure 2 online). Sequence analyses confirmed that *Solanaceous* (potato and tomato) BSL1s are the putative orthologs of *Arabidopsis* BSL1, a protein phosphatase involved in brassinosteroid (BR) signal transduction (see Supplemental Figures 3 and 4 and Supplemental Data Set 2 online) (Mora-García et al., 2004; Kim et al., 2009).

We also used Y2H analysis to confirm that the potato ortholog of *Arabidopsis* BSL1, St-BSL1, interacts with AVR2 (Figure 1B). Gilroy et al. (2011) reported that avirulent isolates of *P. infestans* possess two alleles of AVR2, $AVR2^{K31}$ and $AVR2^{N31}$, that differ in a single amino acid in the N terminus at position 31 prior to the effector domain. In Y2H assays, both AVR2 alleles interacted with potato St-BSL1 (Figure 1B). The Y2H assays also confirmed that the C-terminal effector domain of AVR2 (amino acids 66 to 116) is sufficient for interaction with BSL1 (Figure 1B).

In summary, the co-IP and Y2H experiments provided independent evidence that the RXLR effector AVR2 of *P. infestans*

as a negative control. The RXLR effector PITG_08949, which is closely related to AVR2 across the N-terminal translocation domain but which differs across the C-terminal effector domain due to a likely recombination event (Gilroy et al., 2011), did not interact with St-BSL1 using Y2H analysis.

A

FLAG:AVR2

SlBSL1^Kelch:GFP	–	+	–	–
SlBSL1^Phospho:GFP	–	–	+	–
SlBSL1:GFP	–	–	–	+

input

KD
170
130
100
70
55
40
35
25

α-GFP

10
FLAG:AVR2

α-FLAG

Rubisco

PS

GFP IP

170
130
100
70
55
40
35
25

α-GFP

10
FLAG:AVR2

α-FLAG

FLAG IP

130
100
70
55

SlBSL1:GFP
SlBSL1^Phospho:GFP

α-GFP

10
FLAG:AVR2

α-FLAG

B

29 107
94 158   519   878   Associates with AVR2?

SlBSL1:GFP   ✓
SlBSL1^Kelch:GFP   ✗
SlBSL1^Phospho:GFP   ✓

⊢—⊣ 100 amino acids

▦ Kelch domain   ▮ Phosphatase domain   ▮ GFP

Figure 2. Immunoblots Showing AVR2 Specifically Associates with the Putative Phosphatase Domain of Sl-BSL1 in Planta.

(A) FLAG:AVR2 was transiently expressed alone, with SlBSL1^Kelch:GFP, SlBSL1^Phospho:GFP, or SlBSL1:GFP in *N. benthamiana*. Immunoprecipitates (IP) obtained with anti-FLAG or anti-GFP antiserum and total protein extracts were immunoblotted with appropriate antisera. The expected sizes of the GFP fusion proteins are indicated by red dots in the crude extracts and GFP co-IP probed with anti-GFP antibody. PS, Ponceau stain; Rubisco, ribulose-1,5-bisphosphate carboxylase/oxygenase.
(B) Schematic illustrating the regions of Sl-BSL1 used to assess interaction with AVR2. Numbers indicate position of the amino acid residues.

interacts with the plant protein phosphatase BSL1. AVR2 interacts with BSL1 orthologs from the two major host species of *P. infestans*, tomato, and potato.

### AVR2 Interacts with the Putative Phosphatase Domain of BSL1

To determine which part of BSL1 interacts with AVR2, we cloned the region upstream of the putative phosphatase domain (amino acids 1 to 519) and the putative phosphatase domain (amino acids 520 to 878) and fused these fragments to the GFP at the C terminus. Using co-IPs, we demonstrated an association between the putative phosphatase domain of Sl-BSL1 and AVR2 in planta (Figure 2). Y2H analysis also illustrated that the putative phosphatase domain of St-BSL1 was sufficient for inducing an interaction with AVR2 in vivo (see Supplemental Figure 5 online).

AVR2 Localizes around *P. infestans* Haustoria

To investigate the spatial distribution of AVR2, we expressed a GFP:AVR2 fusion protein (see Supplemental Figure 1B online) in *N. benthamiana* and assessed the intracellular localization by confocal microscopy. GFP:AVR2 accumulated at the cell periphery and, to a lesser extent, within the cytoplasm and nucleus (see Supplemental Figure 6A online). To investigate this further, we coexpressed GFP:AVR2 with a Remorin red fluorescent protein (RFP) fusion. Remorin is a plant protein that accumulates in lipid rafts of the plasma membrane (Raffaele et al., 2009). GFP:AVR2 and RFP:StRemorin largely colocalized at the plasma membrane in planta (see Supplemental Figure 7 online). However, the AVR2 GFP signal was also detected within the nucleus and at low levels within the cytoplasm, which may be due to partial cleavage of the GFP:AVR2 fusion protein (see Supplemental Figure 6B online). Similar results were obtained from the localization of the AVR2 homolog PEXRD11 in planta (see Supplemental Figure 7 online).

To investigate the intracellular localization of AVR2 during infection, we inoculated *N. benthamiana* leaves expressing GFP:AVR2 with the *P. infestans* strain 88069td that expresses an RFP marker (Bozkurt et al., 2011; Chaparro-Garcia et al., 2011). Infected plant cells were identified under bright-field microscopy by the presence of *P. infestans* haustoria. Remarkably, we observed that the GFP:AVR2 signal was altered in infected cells with preferential accumulation around haustoria (perihaustorial localization) (Figure 3A).

To investigate further the localization of AVR2 during infection, we coexpressed AVR2 with the *P. infestans* plasma membrane–associated perihaustorial effector AVRblb2 (Bozkurt et al., 2011). GFP:AVR2 and RFP:AVRblb2 fusion proteins were coexpressed in *N. benthamiana* and their spatial distribution assessed by confocal microscopy. The GFP:AVR2 and RFP:AVRblb2 fluorescent signals overlapped in planta, supporting that AVR2 localizes, at least partially, to the plasma membrane (see Supplemental Figure 8 online). When leaves expressing GFP:AVR2 and RFP:AVRblb2 were inoculated with *P. infestans*, the two signals preferentially coaccumulated around haustoria, further supporting perihaustorial localization of AVR2 (Figure 3B).
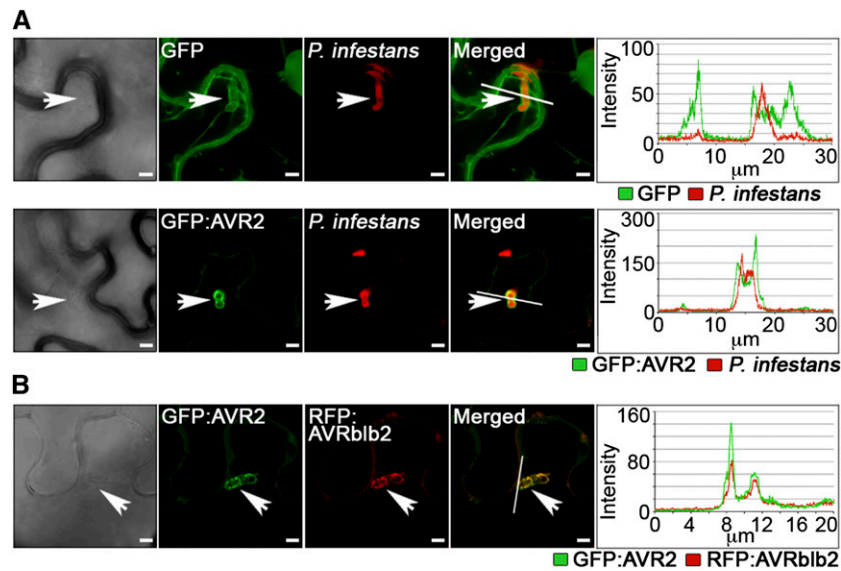
Figure 3. *P. infestans* AVR2 Accumulates around Haustoria and Colocalizes with the Perihaustorial-Localized Effector AVRblb2 in Planta.

(A) *P. infestans* (red)–infected *N. benthamiana* cells preferentially accumulated transiently expressed GFP:AVR2 (green) around haustoria (arrowheads) when compared with the localization of GFP alone.

(B) *P. infestans*–infected cells accumulated GFP:AVR2 and RFP:AVRblb2 at sites of haustorial penetration (arrowheads), illustrated by overlapping peaks of fluorescence intensity.

Pictures were taken at 4 DAI. Bars = 5 µm.

BSL1 Colocalizes with AVR2 in Planta and during Infection

To examine the spatial distribution of BSL1 in planta, we expressed a SlBSL1:GFP fusion protein in *N. benthamiana*. The fluorescent signal for SlBSL1:GFP was excluded from the nucleus and detected at the cell periphery and within the cytoplasm (Figure 4A). To determine whether Sl-BSL1 localized at the plasma membrane, we coexpressed SlBSL1:GFP with RFP:StRemorin in *N. benthamiana*. The two fluorescent signals largely overlapped, indicating partial plasma membrane association of Sl-BSL1, as has been described previously for At-BSL1 (Benschop et al., 2007; Kim et al., 2009). However, following salt-induced plasmolysis, the signals were quite distinct, indicating that Sl-BSL1 only partially localized at the plasma membrane in planta (see Supplemental Figure 7 online).

To determine whether AVR2 and Sl-BSL1 colocalize in planta, we coexpressed GFP:AVR2 and SlBSL1:RFP fusion proteins in *N. benthamiana*. We observed a clear overlap in the two fluorescent protein signals in planta (Figure 4B). When *N. benthamiana* leaves expressing GFP:AVR2 and SlBSL1:RFP were inoculated with *P. infestans*, the two fluorescent signals colocalized at the sites of haustorial penetration indicating perihaustorial localization of both proteins (Figure 4C).

Similar results were obtained from the localization of the AVR2 homolog PEXRD11 in planta. We observed perihaustorial accumulation of GFP:PEXRD11 and colocalization with AVRblb2 around haustoria in infected *N. benthamiana* cells (see Supplemental Figure 9 online). GFP:PEXRD11 also colocalized with SlBSL1:RFP in planta and at haustoria in cells infected with *P. infestans* (see Supplemental Figure 10 online).

To investigate the potential interaction of AVR2 and BSL1 at the observed sites of colocalization, we used bimolecular fluorescence complementation. The N terminus of yellow fluorescent protein (YFP; YN) was fused to full-length AVR2^{N31} or AVR2^{K31} (minus the signal peptide region) and coexpressed with the C terminus of YFP fused to St-BSL1 in *N. benthamiana*. Using confocal microscopy, fluorescence was detected at the cell periphery and in the cytoplasm, but excluded from within the nucleus, supporting interaction between AVR2 and BSL1 at these sites (see Supplemental Figure 11 online).

AVR2 Homologs That Are Recognized by R2 Associate with BSL1

AVR2 belongs to a large family of RXLR effectors from *P. infestans* with highly divergent amino acid sequences (ranging from 28 to 98% in identity between family members) that are differentially recognized by wild potato R2 protein (Haas et al., 2009; Champouret, 2010). Therefore, we extended our study to determine if BSL1 could associate with other members of this family. AVR2 and PEXRD11 belong to RXLR families 7 and 32 according to the classification of Haas et al. (2009). Of these families, 13 RXLR effectors have divergent sequences yet share similarity to AVR2 in their C-terminal domains (Champouret, 2010). We coexpressed these family members as FLAG-tagged fusion proteins with SlBSL1:GFP in *N. benthamiana* and performed co-IPs using an anti-FLAG antibody. Co-IP analysis was inconclusive for three family members (PITG_05121, PITG_15972, and PITG_13936) as these FLAG-tagged fusion proteins displayed reduced stability in planta. Of the remaining
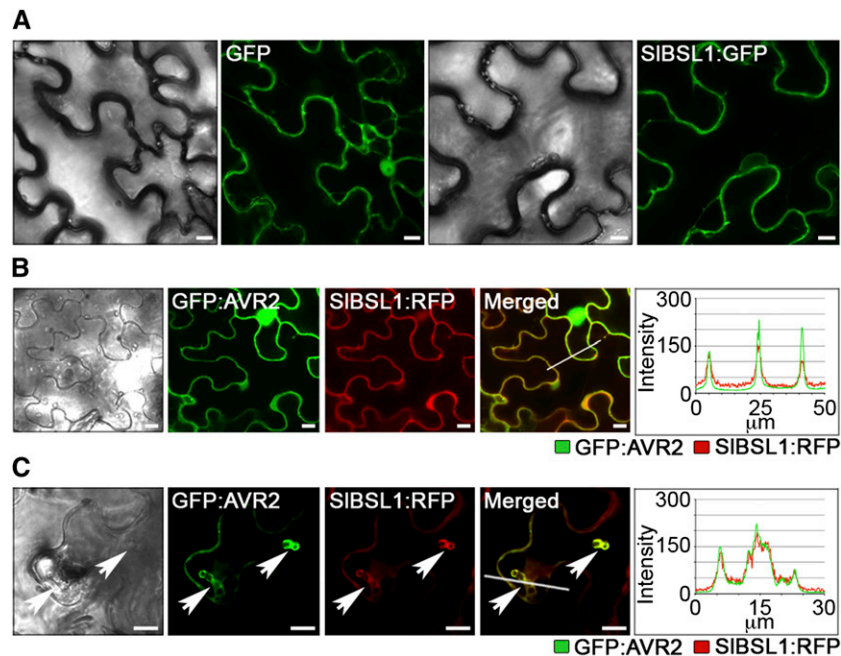
Figure 4. Sl-BSL1 and *P. infestans* AVR2 Colocalize and Accumulate around Haustoria in Planta.

(A) Transient expression of SlBSL1:RFP in *N. benthamiana* reveals that Sl-BSL1 is excluded from the nucleus and localizes at the cell periphery and within the cytoplasm.

(B) Transient expression of GFP:AVR2 and SlBSL1:RFP fusion proteins revealed similar patterns of localization for the two markers, accumulating at the cell periphery, as shown by overlapping peaks in fluorescence intensity. GFP:AVR2 was also detected in the nucleus.

(C) GFP:AVR2 and SlBSL1:RFP localize strongly at sites of *P. infestans* haustorial penetration in *N. benthamiana*.

Pictures were taken at 3 DAI. Bars = 10 μm.

10 family members, we found that only five associated with Sl-BSL1 (Figure 5). Remarkably, four AVR2 homologs that associate with Sl-BSL1 (AVR2, PEXRD11, PITG_21949, and PITG_21645) are the same effectors that were previously shown to activate R2 (Champouret, 2010). A fifth AVR2 homolog, PITG_13940, also associated with Sl-BSL1 and was found to activate R2 in our assays, when infiltrated at higher concentrations than used by Champouret (2010) (see Supplemental Figure 12 online). This shows a correlation between the AVR2 family members that associate with BSL1 and their recognition by R2 and raises the possibility that BSL1 plays a role in R2 recognition of AVR2.

BSL1 Is Specifically Required for R2-Mediated Recognition and Resistance

To determine the extent to which BSL1 is involved in AVR2-R2 recognition, we performed VIGS of Nb-*BSL1* (see Supplemental Figure 13 online) in *N. benthamiana*. To reduce the potential for off-target silencing, we selected a 290-bp fragment of the kelch repeat domain and a 300-bp region of the phosphatase domain of Nb-*BSL1* and expressed them in the tobacco rattle virus (TRV) VIGS-based silencing system (see Supplemental Figure 13A online) (Ratcliff et al., 1999). While sequences encoding these regions are found in other genes, the combination of kelch-repeat and phosphatase domains is only found in members of the *BSL* family.

Plants expressing the TRV:*NbBSL1* constructs did not show any marked phenotypic alterations and were comparable to the TRV:*GFP* control plants (see Supplemental Figure 13B online). Using quantitative RT-PCR, we observed a reduction in the accumulation of Nb-*BSL1* transcripts only in plants infected with the two TRV:*NbBSL1* constructs. To ensure that silencing of *BSL1* was specific and did not affect transcript levels of related genes, we monitored the expression of *BSL2*, the closest paralog based on the recently released genome sequence draft of *N. benthamiana* (http://solgenomics.net/organism/Nicotiana_benthamiana/genome; see Methods). Unlike the observed decrease in *BSL1* transcripts, TRV:*NbBSL1* inoculations failed to affect the accumulation of *BSL2* transcripts (see Supplemental Figures 13C and 13D online).

We coexpressed AVR2 with R2 and three additional R2 family members (R2-like, Rpi-abpt, and Rpi-blb3) that have the same recognition specificity (Lokossou et al., 2009) in *BSL1*-silenced plants and monitored development of the HR. We found that *BSL1* silencing, using either TRV:*NbBSL1* construct, significantly reduced recognition of AVR2 by all four R2 orthologs (Figure 6A). To ensure that the observed reduction in HR was not due to pleotropic effects from silencing of *BSL1*, we also confirmed that R2 was stable in *BSL1*-silenced plants (see Supplemental Figure 13E online).

To determine whether *BSL1* silencing affects other AVR–R interactions, we coexpressed three additional AVR-R combinations,
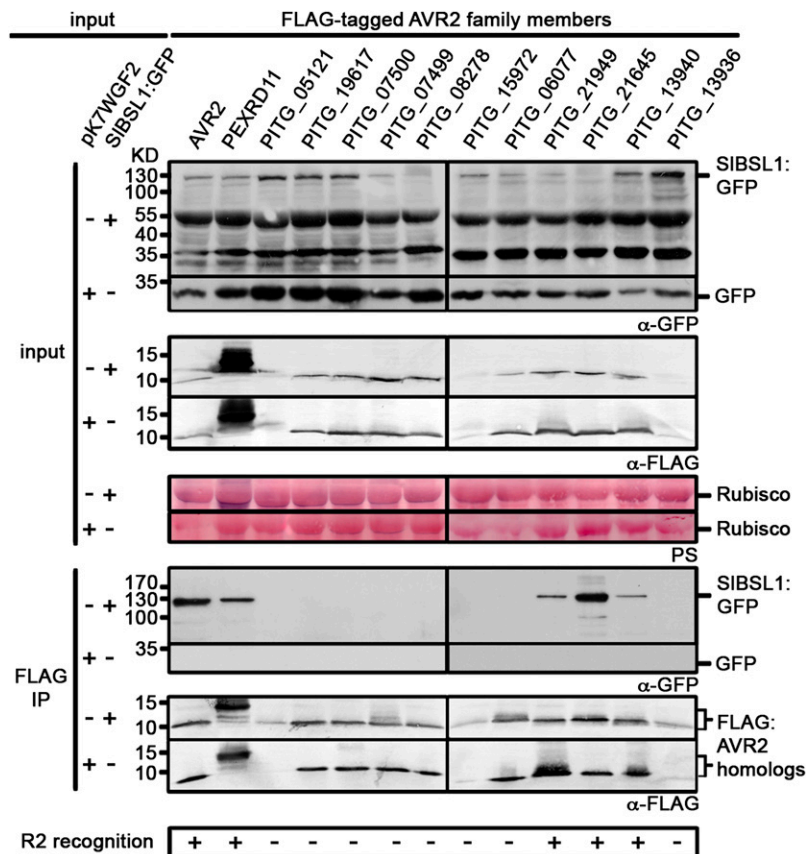
Figure 5. Immunoblots Showing That Five of the 13 AVR2 Family Members Associate with Sl-BSL1 and Activate R2-Mediated Recognition.

FLAG-tagged protein fusions of AVR2 family members were transiently expressed with pK7WGF2 or SlBSL1:GFP in *N. benthamiana*. Immunoprecipitates obtained with anti-FLAG or anti-GFP antiserum and total protein extracts were immunoblotted with appropriate antisera. IP, immunoprecipitate; PS, Ponceau stain.

[See online article for color version of this figure.]

AVR3a/R3a (Armstrong et al., 2005), IPI-O/Rpi-sto1 (Champouret et al., 2009), and PVX-CP/Rx (Moffett et al., 2002), in leaves of *BSL1*-silenced *N. benthamiana*. Silencing of *BSL1* did not affect the HR triggered by these other AVR–R interactions (Figures 6A and 6B). Also, we did not observe cell death following expression of either effectors (AVR3a, PVX-CP, and ipiO1) or corresponding resistance proteins (R3a, Rx, and Sto1) alone in *BSL1*-silenced plants (see Supplemental Figure 13F online). In conclusion, BSL1 is required specifically for the recognition of AVR2 by R2 among the AVR-R pairs we examined.

To determine whether silencing of *BSL1* perturbs R2-mediated resistance to *P. infestans*, we infected *BSL1*-silenced plants transiently expressing R2 with *P. infestans* (Figures 6C and 6D). First, we expressed R2 and, as a control, the resistance protein Rpi-sto1 in each half of the same leaf (total 60 leaves each) from *BSL1*-silenced and TRV:*GFP* plants through agroinfiltration. Next, we infected these leaves with the *P. infestans* strain 88069, which expresses recognized forms of both *Avr* effector genes (*Avr2* and *Avrblb1*). In leaf panels that transiently expressed R2, we observed a significant increase in the number of sites showing late blight lesions in the *BSL1*-silenced plants

compared with TRV:*GFP* plants (Figures 6C and 6D). By contrast, in leaf panels expressing Rpi-sto1, the number of sites with sporulating lesions remained low in both *BSL1*-silenced and TRV:*GFP* plants, indicating Rpi-sto1–mediated resistance was not affected. We conclude that silencing of *BSL1* specifically compromises R2-mediated resistance to *P. infestans*. However, silencing of *BSL1* did not alter the compatible interaction with *P. infestans* in the absence of R2 (see Supplemental Figure 14 online).

AVR2 Promotes the Interaction between BSL1 and R2

Given that BSL1 is required for R2-mediated recognition of AVR2, a logical step was to investigate whether these proteins associate in planta. To elucidate this, we performed co-IP experiments involving a GFP-tagged R2 protein (GFP:SdR2), FLAG-tagged AVR2 protein (FLAG:AVR2), and a myc-tagged BSL1 protein (SlBSL1:myc) in different combinations (Figure 7). These constructs were expressed in *N. benthamiana* using agroinfiltration. Co-IPs with anti-GFP antibodies resulted in the recovery of Sl-BSL1 only in the presence of AVR2 expression
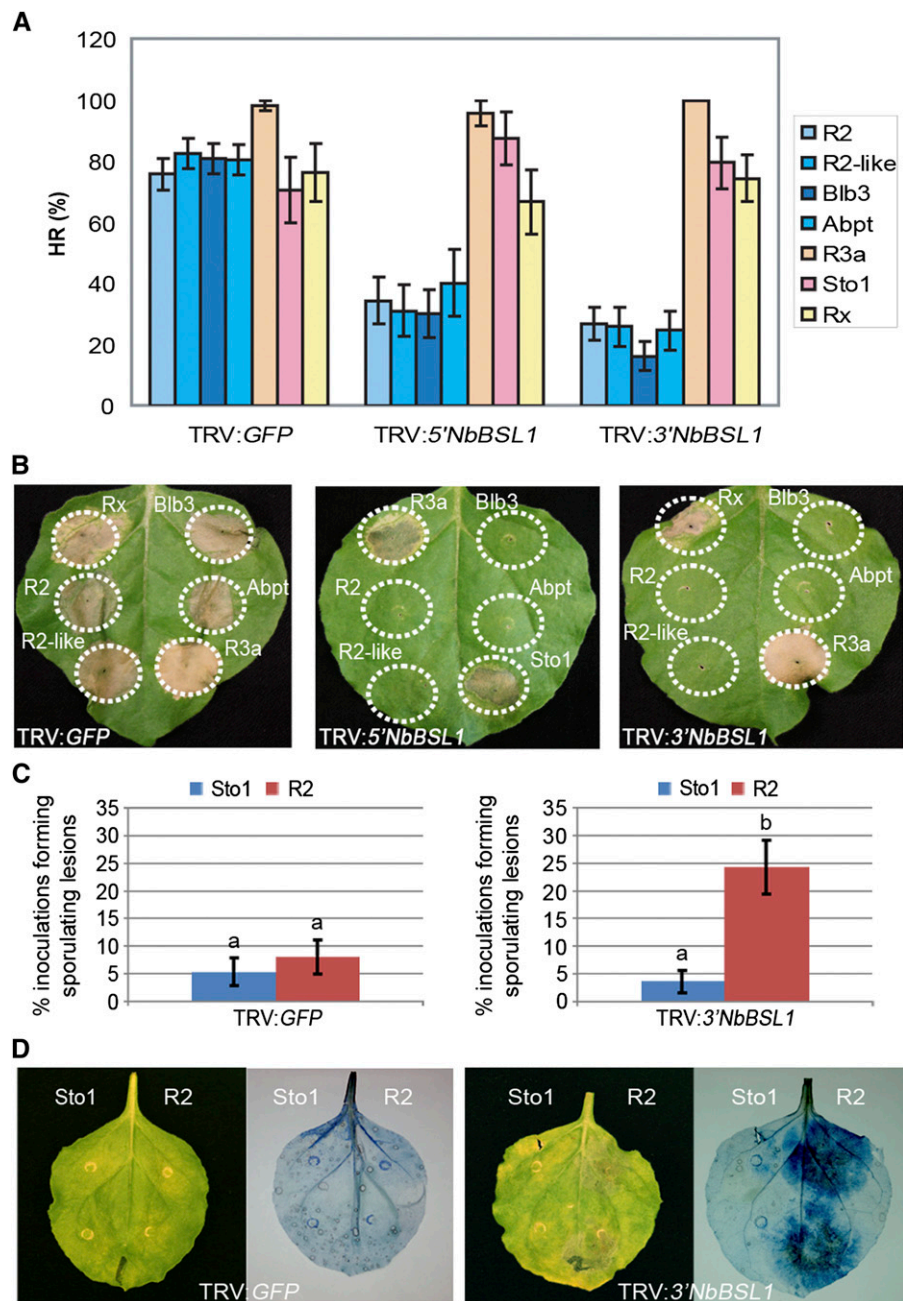
Figure 6. BSL1 Expression Is Required for R2-Mediated Recognition and Resistance.

(A) and **(B)** VIGS of Nb-*BSL1* specifically perturbed R2-mediated hypersensitivity (HR). AVR-R combinations were coexpressed (only the R proteins are indicated in the figure) in *N. benthamiana* using agroinfiltration. HR (%) indicates the percentage of infiltration sites showing a confluent zone of cell death.

(C) and **(D)** VIGS of Nb-*BSL1* inhibited R2-mediated resistance. Growth of *P. infestans* (also visualized by trypan blue staining) was significantly increased on *BSL1*-silenced plants transiently expressing R2 when compared with Rpi-sto1 expression. Letter "b" indicates a significant difference (P < 0.001) in the mean number of plants that show infection following R2 treatment, compared with Sto1 treatment ("a") on TRV:*3'NbBSL1* plants, using logistical regression analysis. Error bars represent ± sᴇ.

(Figure 7). The same co-IPs failed to recover AVR2. However, co-IPs performed with anti-FLAG antibodies revealed a weak GFP reacting signal corresponding to R2 (Figure 7). This indicates that, although we have obtained no evidence for an exclusive direct interaction between AVR2 and R2, these two proteins may associate through a ternary complex with BSL1 that forms in planta (Figure 7). This observation was also confirmed by Y2H analysis, which failed to demonstrate a direct interaction between AVR2 and R2 (see Supplemental Figure 15 online).

The Stealthy A2L Variant Associates with BSL1

Strains of *P. infestans*, such as those from the virulent clonal lineage 13_A2, that are virulent on R2 potatoes, express the A2L variant that evades perception by R2 (Gilroy et al., 2011). To determine whether A2L interacts with BSL1, we expressed a FLAG-tagged C-terminal region of A2L (amino acids 66 to 116) and SlBSL1:GFP in *N. benthamiana* by agroinfiltration. Co-IP analysis revealed that the FLAG:A2L protein associates with Sl-BSL1 (Figure 8A). We also demonstrated the direct interaction of the full-length (minus signal peptide) and C-terminal domain (amino acids 66 to 116) of A2L with St-BSL1 by Y2H analysis (Figure 8B).

A2L Does Not Promote the Interaction between BSL1 and R2

Given that AVR2 promotes the association of BSL1 with R2, we investigated whether the virulent form A2L could also promote this association. We coexpressed FLAG:A2L, SlBSL1:myc, and GFP:SdR2 in *N. benthamiana* by agroinfiltration and performed co-IPs as described earlier for AVR2. Co-IPs with GFP antibodies did not recover Sl-BSL1 in the presence of A2L, in sharp contrast with the AVR2 co-IPs (Figure 8C). Therefore, although A2L can associate with BSL1, it differs from AVR2 by not promoting the interaction of BSL1 with R2.

DISCUSSION

Plant NB-LRR receptors can recognize specific pathogen effectors by direct binding or indirectly via plant proteins that are targeted by the effectors. So far, all cases of indirect recognition by NB-LRR proteins have involved bacterial and viral plant pathogens, although these immune receptors can perceive pathogens as diverse as fungi, oomycetes, nematodes, and insects (Rafiqi et al., 2009). Here, we show using co-IP and Y2H that AVR2 and R2 may associate through a ternary complex with the host protein BSL1. Our localization studies indicate that AVR2 and BSL1 share overlapping spatial distributions, which further supports their potential for interaction. We found that the putative plant phosphatase BSL1 is required for R2-mediated perception of the *P. infestans* RXLR effector AVR2 and resistance to an avirulent strain of the late blight pathogen. AVR2 associates with BSL1 and mediates the interaction of BSL1 with R2 in planta. Strains of *P. infestans* that are virulent on R2 potatoes express an unrecognized form, *A2L* (Gilroy et al., 2011).
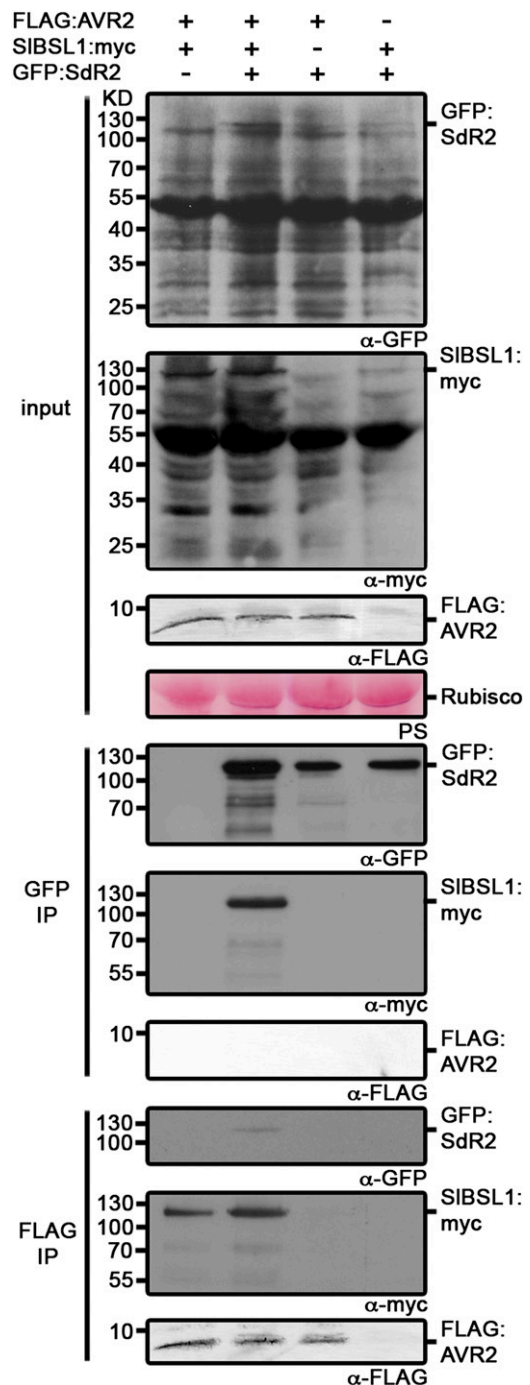
Figure 7. Immunoblots Showing That AVR2 Expression Is Required for Interaction of Sl-BSL1 with R2.

FLAG:AVR2, SlBSL1:myc, and GFP:SdR2 were transiently expressed in combination in *N. benthamiana*. Immunoprecipitates obtained with anti-FLAG or anti-GFP antiserum, and total protein extracts were immunoblotted with appropriate antisera. IP, immunoprecipitate; PS, Ponceau stain; Rubisco, ribulose-1,5-bisphosphate carboxylase/oxygenase.
[See online article for color version of this figure.]
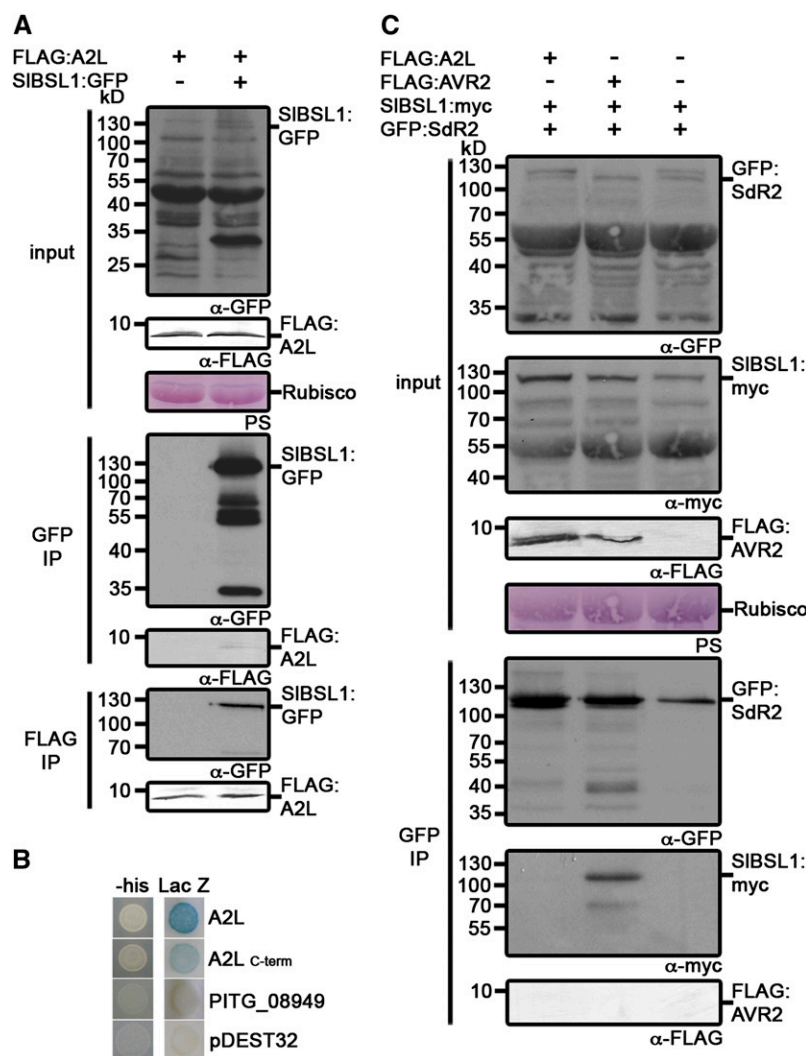
Figure 8. A2L Associates with BSL1 but Does Not Promote an Interaction between BSL1 and R2.

(A) Immunoblots showing A2L coimmunoprecipitates with tomato BSL1 in planta. FLAG:A2L was transiently expressed alone or with SlBSL1:GFP in *N. benthamiana*. Immunoprecipitates obtained with anti-FLAG or anti-GFP antiserum and total protein extracts were immunoblotted with appropriate antisera. IP, immunoprecipitate; Rubisco, ribulose-1,5-bisphosphate carboxylase/oxygenase.

(B) Y2H analysis demonstrating that A2L (excluding the signal peptide) and the C-terminal effector domain of A2L (amino acids 66 to 116) interact with potato BSL1 (St-BSL1) in vivo. Both *LacZ* (blue color) and *His3* (providing growth on medium lacking His [-his]) reporter genes were activated. Empty vector (pDEST32) and effector PITG_08949 (Gilroy et al., 2011) acted as negative controls (no reporter activity).

(C) Immunoblots showing A2L does not promote interaction of Sl-BSL1 with R2. FLAG:A2L, SlBSL1:myc, and GFP:SdR2 were transiently expressed in combination in *N. benthamiana*. Immunoprecipitates obtained with anti-FLAG or anti-GFP antiserum and total protein extracts were immunoblotted with appropriate antisera. PS, Ponceau stain.

A2L also interacts with BSL1 but does not promote the association of BSL1 with R2.

Our objective was to understand how members of the *P. infestans* AVR2 effector family differentially activate R2-mediated hypersensitivity. Our findings point to a model in which any of an AVR2-modified BSL1, a BSL1-modified AVR2, or a AVR2-BSL1 complex interacts with and activates R2 (Figure 9). The stealthy effector A2L still interacts with BSL1, but this association does not lead to R2 activation. One possibility is that AVR2 induces conformational and/or biochemical changes in BSL1 and that

the modified BSL1 protein can now associate with the R2 receptor to activate defense responses. Similar mechanisms of action have been reported for the recognition of bacterial effectors by NB-LRR proteins (Collier and Moffett, 2009; Elmore et al., 2011). For instance, *P. syringae* AvrB and AvrRpm1 promote the phosphorylation of the accessory host protein RIN4, which is perceived by the NB-LRR protein RPM1, resulting in its activation (Chung et al., 2011). By contrast, RPS2 perceives the proteolytic cleavage of RIN4 by *P. syringae* effector AvrRpt2 (Belkhadir et al., 2004). Future work will determine the nature of

any potential conformational and/or biochemical modifications of BSL1 that could be triggered by AVR2 and how the modified BSL1 promotes interaction with R2 and activates R2 immune signaling.

The association of AVR2 with BSL1, the requirement of AVR2 for association of R2 with BSL1, and our inability to detect direct interaction between R2 and AVR2 are compatible with indirect recognition, with BSL1 acting as an intermediary host protein that interacts with both the effector protein and NB-LRR immune receptor. To date, the only reported case of indirect recognition for filamentous plant pathogens is the recognition of the *Cladosporium fulvum* apoplastic effector Avr2 by tomato Cf-2. *C. fulvum* Avr2 selectively inhibits two papain-like Cys proteases, RCR3 and PIP1, which are transcriptionally upregulated by the salicylic acid–regulated defense pathway (Rooney et al., 2005; Shabab et al., 2008). Although the interaction of the *C. fulvum* Avr2 with RCR3 has been demonstrated (Rooney et al., 2005), there is no evidence for association of RCR3 or PIP1 with Cf-2. Therefore, our study represents a clear example of a host protein that associates with both a filamentous plant pathogen effector and its corresponding NB-LRR immune receptor.

Our interpretation of BSL1-mediated indirect recognition of AVR2 contrasts sharply with examples of direct perception of filamentous pathogen effectors by NB-LRR proteins. Examples include the perception of *Magnaporthe oryzae* AVR-Pita effector by the rice (*Oryza sativa*) Pi-ta protein, flax rust *Melampsora lini* AvrL567 by flax L proteins, *H. arabidopsidis* ATR1 by *Arabidopsis* RPP1, and *P. infestans* effector ipiO (Avr-blb1) by the coiled-coil domain of RB (Blb1) (Jia et al., 2000; Dodds et al., 2006; Krasileva et al., 2010; Chen et al., 2012). By contrast, in bacterial systems, effectors are often recognized indirectly with

only one case of direct perception of a bacterial effector by an NB-LRR receptor reported (Deslandes et al., 2003), indicating that the predominant mechanism of plant perception for different classes of pathogens may differ.

The host target of AVR2, BSL1, and its close homolog in *Arabidopsis*, BSU1, have been shown to promote BR signal transduction actively (Kim et al., 2009). Proteomic analysis in *Arabidopsis* showed that BSL1 is a plasma membrane protein, and live-cell imaging revealed that BSL1 is also observed in the cytoplasm (Benschop et al., 2007; Kim et al., 2009). This supports a potential role and site of action for BSL1 in upstream BR signaling events at the cell surface (Kim et al., 2009). Our results indicate that solanaceous BSL1 may also associate with the plasma membrane and cytoplasm in *N. benthamiana* (Figure 4). Similar to the *Arabidopsis* T-DNA knockouts of *BSL1*, which are indistinguishable from wild-type plants due to the functional redundancy between members of the BSL family (Mora-García et al., 2004), silencing of *BSL1* in *N. benthamiana* revealed no striking developmental phenotype (see Supplemental Figure 13B online). Whether or not BSL1 is a positive regulator of BR signaling in solanaceous plants remains to be determined. In addition, silencing of *BSL1* had no impact upon the compatible interaction between *N. benthamiana* and *P. infestans*. However, given the documented functional redundancy between BSL family members in the context of BR signal transduction in *Arabidopsis*, this may also explain an unaltered virulence phenotype when silencing *BSL1* alone in this study. Elucidating the function of BSL1 and how it is perturbed by AVR2, and, indeed, whether AVR2 interacts with and modifies other members of the BSL family, will be necessary to establish whether BSL1 is acting as a guardee or decoy during recognition of *P. infestans* by R2.

Late blight is the most destructive disease of potato, the third most important food crop in the world. *P. infestans* continues to cost modern agriculture billions of dollars annually and is a critical constraint for subsistence potato farming. The most sustainable strategy to manage late blight is to breed broad-spectrum disease resistance into potato. The *R2* gene has been exploited in agriculture (Gilroy et al., 2011; Vleeshouwers et al., 2011). But although virulent races of the pathogen, including the epidemic clonal lineage blue13, have emerged, R2 potatoes have been reported to confer a degree of resistance to local *P. infestans* populations in China, Russia, France, and The Netherlands (Vleeshouwers et al., 2011). Our gained understanding of the mechanism of recognition of *P. infestans* by R2 should prove helpful in managing and improving R2-mediated late blight resistance. For example, synthetic *R2* mutant genes with expanded pathogen recognition specificities could be generated to enhance the spectrum and durability of late blight resistance or to extend recognition to effectors from other pathogens that may also target and modify BSL1 (Vleeshouwers et al., 2011).
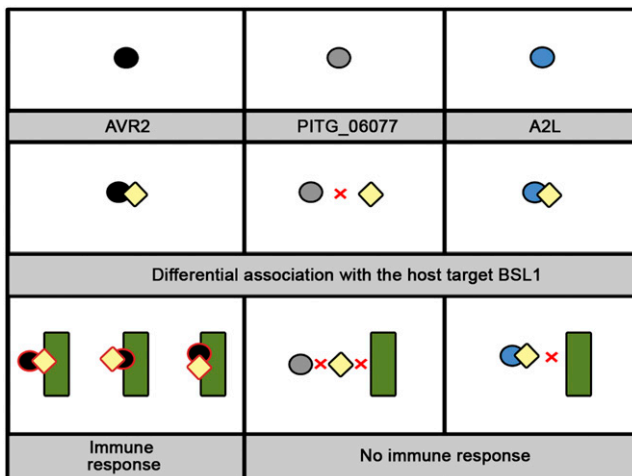
Figure 9. Models Illustrating the Potential Link between Association of AVR2 Family Members with BSL1 and R2-Mediated Recognition and Resistance.

Activation of R2 by AVR2 could be mediated by an AVR2-modifed BSL1, BSL1-modified AVR2, or AVR2-BSL1 complex (left to right). Circles, corresponding effectors; yellow diamonds, BSL1; green rectangles, R2. Potential modifications are indicated by red highlighting.

METHODS

Plasmid Construction and Preparation

All primers used in this study are listed in Supplemental Table 2 online. The C-terminal effector domain of each *Avr2* family member and *A2l* were

custom synthesized with an N-terminal FLAG-tag in place of the signal peptide and RXLR-ERR region, or for PEXRD11 just the signal peptide region, by Genscript and subcloned into the *Tobacco mosaic virus*–based *Agrobacterium tumefaciens* binary vector pTRBO (Lindbo, 2007) (see Supplemental Figure 1A online). All Gateway cloning was performed following the manufacturer's instructions (Invitrogen). *GFP:Avr2* and *GFP:PexRd11* constructs were generated as follows: The full-length *Avr2* gene (excluding the N-terminal signal peptide region; see Supplemental Figure 1B online) and the C-terminal domain of *PexRd11* (following the RXLR-EER motif; see Supplemental Figure 1B online) were generated by PCR using primer combinations 5AVR2/3AVR2 or 5RD11/3RD11 and genomic DNA from *Phytophthora infestans* isolate 88069. These amplicons were then cloned into the entry vector pENTR/D-TOPO (Invitrogen) and resulting clones confirmed by sequencing. The entry clone inserts were then introduced into pK7WGF2 (Karimi et al., 2002) by Gateway LR recombination (Invitrogen). Initially constructs were designed both with and without the RXLR region. However, we now know that the RXLR domain has no impact on the observed localization patterns.

BSL1, *Catalase 1*, and *thioredoxin peroxidase* were cloned into pENTR/D-TOPO (Invitrogen) using the PCR products amplified from tomato (*Solanum lycopersicum*), *Nicotiana benthamiana*, or *Nicotiana tabacum* cDNA, respectively, using primers 5BSL1/3BSL1, 5Cat1/3Cat1, or 5Thper/3Thper. GFP fusions of the three amplicons were generated by Gateway LR recombination of pENTR:*BSL1* with pK7FWG2 and pENTR:*Catalase 1* or pENTR:*thioredoxin* with pK7WGF2 (Karimi et al., 2002). RFP and 4xmyc fusions of *BSL1* were generated by Gateway LR recombination of pENTR:*BSL1* with pGWB554 (*BSL1:RFP*) or pGWB17 (*BSL1:myc*) (Nakagawa et al., 2007). The region upstream of the BSL1 phosphatase domain and the phosphatase domain were cloned into pENTR/D-TOPO (Invitrogen) using the PCR products amplified from tomato (*Solanum lycopersicum*), using primers 5BSL1/3BSL1_kel or 5BSL1_phos/3BSL1. GFP fusions of the two amplicons were generated by Gateway LR recombination of pENTR:*BSL1^Kelch* and pENTR:*BSL1^Phospho* with pK7FWG2.

RFP:AVRblb2 was previously described (Bozkurt et al., 2011). RFP:StRemorin was generated by cloning the PCR amplicon produced using potato (*Solanum tuberosum*) cDNA as a template with primers FStrem13/RStrem13. The amplicon was then used as a template in a second PCR with attB-specific primers and the amplicon cloned into pDONR201. The resulting entry clone insert was then introduced into pGWB555 by Gateway LR recombination.

GFP:SdR2 and *YFP:SdR2* were generated by cloning the PCR amplicon produced using pKGW-MG:*R2* as a template (Lokossou et al., 2009) with primers 5Nterm_R2/3Nterm_R2 into the entry vector pENTR/D-TOPO. The resulting entry clone insert was then introduced into pK7WGF2 or pB7WGY2 (Karimi et al., 2002) by Gateway LR recombination and into pDEST32 and pDEST22 vectors for Y2H analyses.

The Y2H DNA binding domain and activation domain fusions of AVR2 and an activation domain fusion of BSL1 were generated as follows. First, pDNR221 entry clones containing AVR2^K31, AVR2^N31, A2L, the C-terminal effector domain of both AVR2 and A2L (amino acids 66 to 116), or the control RXLR effector PITG_08949 (Gilroy et al., 2011) were recombined with pDEST32 and pDEST22 using Gateway LR recombination. Next, St-*BSL1* was PCR amplified from potato cDNA using primers 5StBSL1-1/3StBSL1-1, which contain partial attB sites. The amplicon was then used as template in a second PCR with primers 5StBSL1-2/3StBSL1-2 to complete the attB recombination sites, before cloning into the entry vector pDON201 followed by Gateway LR recombination into pDEST22. The phosphatase domain of St-*BSL1* was amplified and also cloned into pDEST22 using primers 5StBSL1-CT/3StBSL1-1.

Constructs used for VIGS of BSL1 were generated as follows. A 290- and 300-bp fragment of BSL1 was PCR amplified from *N. benthamiana* cDNA using primers 5BSL1-290/3BSL1-290 and 5BSL1-300/3BSL1-300,

respectively (see Supplemental Figure 13A online). Each fragment was then cloned into the TRV-based silencing vector (Ratcliff et al., 1999).

YN:AVR2^N31, YN:AVR2^K31, and YN:PITG_08949 were generated by recombining pDNR221 entry clones containing AVR2^K31, AVR2^N31, or the control RXLR effector PITG_08949 (Gilroy et al., 2011) with vector CL112 (Bos et al., 2010) using Gateway LR recombination. YC:StBSL1 was generated by recombining the pDON201 entry clone containing St-BSL1 into vector CL113 (Bos et al., 2010) using Gateway LR recombination.

Transient Gene Expression Assays

In planta transient expression by agroinfiltration was performed according to methods described previously (Bos et al., 2006). For each of the *Agrobacterium* strains, a final OD_{600} of 0.3 to 0.4 in agroinfiltration medium (10 mM MES, 10 mM $MgCl_2$, and 150 μM acetosyringone, pH 5.6) was used. For the transient coexpression assays, *Agrobacterium* strains carrying the plant expression constructs were mixed in a 1:1 ratio in agroinfiltration medium to a final OD_{600} of 0.4 to 0.6. GFP:SdR2 induced a delayed HR when coinfiltrated with AVR2; therefore, co-IPs were conducted with tissue not displaying HR.

Co-IP Experiments and Immunoblot Analysis

For co-IP experiments, total proteins were extracted from *N. benthamiana* leaves 4 d after agroinfiltration and peptides prepared for LC-MS/MS as described previously (Win et al., 2011). Immunoblot analyses were performed on SDS-PAGE separated proteins as described elsewhere (Oh et al., 2009). Monoclonal FLAG M2-alkaline phosphatase antibodies (Sigma-Aldrich) were used at 1:10,000 dilution and blots developed using the AP conjugate substrate kit (Bio-Rad). The α-GAL4 activation domain monoclonal antibody (Clontech) was used at 1:6000 to detect Sd-R2 protein expression and stability in yeast cells. Polyclonal GFP antibodies (Invitrogen) at 1:4000 and polyclonal myc-antibodies at 1:4000 (Santa Cruz Biotechnology) were used as primary antibodies, and anti-rabbit polyclonal antibody conjugated to horseradish peroxidase (Sigma-Aldrich) was used as a secondary antibody at a dilution of 1:12,000. Protein bands on immunoblots were detected using ECL substrate (Thermo Scientific Pierce) and exposed on Amersham Hyperfilm ECL (GE Healthcare).

Y2H Analyses

pDEST22:*StBSL1* was cotransformed with the pDEST32 constructs containing AVR2^K31, AVR2^N31, A2L, the C-terminal effector domain of both AVR2 and A2L (amino acids 66 to 116), the control RXLR effector PITG_08949, or pDEST32 alone into the yeast strain MaV203. pDEST22:*StBSL1^phospho* (phosphatase domain) was cotransformed with pDEST32 constructs containing AVR2^K31, AVR2^N31, the C-terminal effector domain of AVR2 (amino acids 66 to 116), and the control RXLR effector PITG_08949. pDEST22:*SdR2* and pDEST32:*SdR2* were cotransformed with appropriate effector forms in the corresponding pDEST22 or pDEST32 vectors (as above). Transformed cells were plated out on synthetic complete media lacking Leu and Trp. Colonies were picked from these plates to test interaction in reporter gene assays (the same medium for the *LacZ* assay and the same medium but lacking His for the *HIS3* assay), using the ProQuest system (Invitrogen), following the manufacturer's protocol.

VIGS

VIGS was performed in *N. benthamiana* as described by Peart et al. (2002). A TRV construct expressing GFP was used as a control (Gilroy et al., 2007). To confirm silencing RT-PCR was performed on *BSL1-* and

GFP-silenced plant material 2 to 4 weeks after infection with TRV constructs, to PCR amplify either Nb-*BSL1* using primers 5BSL1-RT/3BSL1-RT or Nb-*BSL2* using primers 5BSL2-RT/3BSL2-RT. Nb-*BSL2* was identified as the closest paralog based on a TBLASTN search of the recently released genome sequence draft of *N. benthamiana* (http://solgenomics.net/organism/Nicotiana_benthamiana/genome) with *Arabidopsis* BSL family members At-BSU1, At-BSL2, and At-BSL3. To assess the stability of YFP:SdR2 in *BSL1*-silenced plants, YFP:SdR2 was transiently expressed in plants expressing each TRV construct and in unsilenced plants. Total proteins were extracted 3 d after infection (DAI) and immunoblot analysis undertaken as described previously (Gilroy et al., 2011).

HR Assays

Following VIGS, transgenes were delivered into *N. benthamiana* leaves by agroinfiltration 2 to 3 weeks after infiltration with the TRV constructs. *Agrobacterium* cultures were resuspended in agroinfiltration medium at a final concentration of OD_{600} 0.4 for those delivering the effector transgenes and OD_{600} 0.75 for those delivering the *R* genes and results recorded and photographed 5 d after infiltration. Following agroinfiltration, HR was monitored as described previously (Gilroy et al., 2011) with six independent biological experiments, each with three leaves per plant, from four plants.

To assess the ability of PITG_13940 to induce R2-mediated HR, pTRBO:AVR2, pTRBO:PEXRD11, and pTRBO:PITG_13940 were transiently coexpressed in *N. benthamiana* with pKGW-MG:R2 (Lokossou et al., 2009) using agroinfiltration.

Agrobacterium Transient Assay

Agrobacterium transient assay was performed on *N. benthamiana* plants following VIGS 3 weeks after initial infiltration with the TRV constructs. First, *Agrobacterium* cultures were resuspended in agroinfiltration medium at a final concentration of OD_{600} 0.3 and used for transient expression in planta by agroinfiltration of the VIGS plants. After 2 d, each infiltration site was inoculated with zoospores from *P. infestans* isolate 88069 as described previously (Bos et al., 2010). Three biological replicates of 20 leaves each were assessed for late blight lesions 6 d after infection (DAI) for each VIGS construct. The percentage of inoculation sites that formed sporulating lesions were compared with the total number of sites inoculated. Leaves were photographed at 5 to 6 DAI. Trypan blue staining was performed as described previously by Gilroy et al. (2007).

P. infestans Infection Assays for Microscopy

Assays to observe the localization of AVR2, PEXRD11, and BSL1 during infection were performed as follows: First *GFP:Avr2*, *GFP:PexRD11*, and/or *BSL1:RFP* were transiently expressed under the 35S promoter in *N. benthamiana* leaves by agroinfiltration. At 48 h after infiltration, the infiltrated leaves were detached and inoculated with the *P. infestans* 88069 or 88069td (100,000 zoospores/mL) strains on six spots for each leaf. Localization of the fluorescent proteins at sites of *P. infestans* haustoria formation was recorded using confocal microscopy 2 to 4 DAI.

Confocal Microscopy

Patches of *N. benthamiana* leaves were cut and mounted in water and analyzed on a Leica DM6000B/TCS SP5 confocal microscope (Leica Microsystems CMS) with the following excitation wavelengths: GFP, 488 nm; RFP, 561 nm. Scanning was performed in sequential mode to prevent signal bleed-through. For bimolecular fluorescence complementation, a Leica SP2 confocal laser scanning microscope on a DM6000 microscope fitted with a Fl/RH filter block and water dipping lenses (HCX APO L10×/0.30 W U-V-1, L20×/0.50 W U-V-1, L40×/0.80 W U-V-1, or L63×/0.90 W U-V-1) was used. YFP fluorescence was collected using excitation at 514 nm with emission collected at 530 to 575 nm using the L40×/0.80 W U-V-1 lens.

Accession Numbers

Sequence data from this article can be found in the GenBank/EMBL databases under the following accession numbers: *Avr2* (*PITG_22870*, XM_002902940.1 and *PITG_08943*, XM_002902939.1), *PexRd11* (*PITG_13930*, XM_002899550.1), *PITG_05121* (XM_002998776.1), *PITG_19617* (XM_002996892.1), *PITG_07500* (XM_002904456.1), *PITG_07499* (XM_002904455.1), *PITG_08278* (XM_002903638.1), *PITG_15972* (XM_002898139.1), *PITG_06077* (XM_002998224.1), *PITG_21949* (XM_002996830.1), *PITG_21645* (XM_002894729.1), *PITG_13940* (XM_002899557.1), *PITG_13936* (XM_002899553.1), *S. lycopersicum BSL1* (JQ886089), *N. tabacum Catalase 1* (JQ886090), *N. tabacum Thioredoxin peroxidase* (JQ886091), *Solanum demissum R2* (FJ536325.1), *S. tuberosum BSL1* (JQ950742) and *BSL2* JQ950743), *N. benthamiana BSL1* (JQ950744), and *N. benthamiana BSL2* (JQ969018).

Supplemental Data

The following materials are available in the online version of this article.

Supplemental Figure 1. Schematic Representation of AVR2 Family Fusion Constructs Used in Co-IPs.

Supplemental Figure 2. Immunoblots Showing That *P. infestans* PEXRD11 Specifically Associates with Sl-BSL1 in Planta.

Supplemental Figure 3. Sequence Analysis Confirms That BSL1 from *Solanum tuberosum* (Potato), *Solanum lycopersicum* (Tomato), and *Nicotiana benthamiana* Are Orthologs of *Arabidopsis* BSL1.

Supplemental Figure 4. *Arabidopsis*, *Solanum tuberosum* (Potato), and *Solanum lycopersicum* (Tomato) BSL1 Full-Length Amino Acid Sequences Are Highly Conserved.

Supplemental Figure 5. Y2H Analysis Illustrating That *P. infestans* $AVR2^{K31}$, $AVR2^{N31}$, and the C-Terminal Effector Domain of AVR2 (Amino Acids 66 to 116) Interact with the Phosphatase Domain (Amino Acids 520 to 881) of Potato BSL1 (St-BSL1) in Vivo.

Supplemental Figure 6. Localization and Stability of *P. infestans* AVR2 in Planta.

Supplemental Figure 7. *P. infestans* AVR2 and PEXRD11 Colocalize with the Plasma Membrane–Associated Protein Remorin in Planta.

Supplemental Figure 8. *P. infestans* AVR2 and PEXRD11 Colocalize with the *P. infestans* Plasma Membrane–Associated Effector AVRblb2 in Planta.

Supplemental Figure 9. *P. infestans* PEXRD11 Accumulates around Haustoria and Colocalizes with the Perihaustorial-Localized Effector AVRblb2 in Planta.

Supplemental Figure 10. Tomato BSL1 and *P. infestans* PEXRD11 Colocalize in Planta and Accumulate around Haustoria.

Supplemental Figure 11. AVR2 Is in Close Proximity to St-BSL1 at the Cell Periphery and within the Cytoplasm.

Supplemental Figure 12. PITG_13940 Activates R2-Mediated Hypersensitivity (HR).

Supplemental Figure 13. Virus-Induced Gene Silencing of *BSL1* in *N. benthamiana*.

Supplemental Figure 14. VIGS of *BSL1* in *N. benthamiana* Did Not Affect Colonization by *P. infestans*.

Supplemental Figure 15. Y2H Analysis Failed to Demonstrate a Direct Interaction between AVR2 and R2.

Supplemental Table 1. Plant Proteins That Specifically Associated with AVR2 Family Effectors after Coimmunoprecipitation as Identified by Mass Spectrometry.

Supplemental Table 2. Details of Primers Used in This Study.

Supplemental Data Set 1. Peptide Matches from Mascot Spectra Searches That Identified Plant Proteins Specifically Associated with AVR2 Family Effectors in Coimmunoprecipitations.

Supplemental Data Set 2. Text File of the Alignment Used for the Phylogenetic Analysis Shown in Supplemental Figure 3.

AUTHOR CONTRIBUTIONS

D.G.O.S., S.B., J.W., S.S., P.R.J.B., E.M.G., and S.K. designed research. D.G.O.S., S.B., J.W., S.S., I.H., T.O.B., and E.M.G. performed research. D.G.O.S., S.B., J.W., S.S., N.C., V.G.A.A.V., P.R.J.B., E.M.G., and S.K. analyzed data. D.G.O.S., S.B., P.R.J.B., and S.K. wrote the article, and all authors commented on the article before submission.

REFERENCES

Armstrong, M.R., et al. (2005). An ancestral oomycete locus contains late blight avirulence gene *Avr3a*, encoding a protein that is recognized in the host cytoplasm. Proc. Natl. Acad. Sci. USA **102:** 7766–7771.

Belkhadir, Y., Nimchuk, Z., Hubert, D.A., Mackey, D., and Dangl, J. L. (2004). *Arabidopsis* RIN4 negatively regulates disease resistance mediated by RPS2 and RPM1 downstream or independent of the NDR1 signal modulator and is not required for the virulence functions of bacterial type III effectors AvrRpt2 or AvrRpm1. Plant Cell **16:** 2822–2835.

Benschop, J.J., Mohammed, S., O'Flaherty, M., Heck, A.J., Slijper, M., and Menke, F.L. (2007). Quantitative phosphoproteomics of early elicitor signaling in *Arabidopsis*. Mol. Cell. Proteomics **6:** 1198–1214.

Bos, J.I., et al. (2010). *Phytophthora infestans* effector AVR3a is essential for virulence and manipulates plant immunity by stabilizing host E3 ligase CMPG1. Proc. Natl. Acad. Sci. USA **107:** 9909–9914.

Bos, J.I., Kanneganti, T.D., Young, C., Cakir, C., Huitema, E., Win, J., Armstrong, M.R., Birch, P.R., and Kamoun, S. (2006). The C-terminal half of *Phytophthora infestans* RXLR effector AVR3a is sufficient to trigger R3a-mediated hypersensitivity and suppress INF1-induced cell death in *Nicotiana benthamiana*. Plant J. **48:** 165–176.

Bozkurt, T.O., Schornack, S., Win, J., Shindo, T., Ilyas, M., Oliva, R., Cano, L.M., Jones, A.M., Huitema, E., van der Hoorn, R.A., and Kamoun, S. (2011). *Phytophthora infestans* effector AVRblb2 prevents secretion of a plant immune protease at the haustorial interface. Proc. Natl. Acad. Sci. USA **108:** 20832–20837.

Champouret, N. (2010). Functional Genomics of *Phytophthora infestans* Effectors and *Solanum* Resistance Genes. PhD dissertation (Wageningen, The Netherlands: Wageningen University), p. 162.

Champouret, N., Bouwmeester, K., Rietman, H., van der Lee, T., Maliepaard, C., Heupink, A., van de Vondervoort, P.J.I., Jacobsen, E., Visser, R.G.F., van der Vossen, E.A.G., Govers, F., and Vleeshouwers, V.G. (2009). *Phytophthora infestans* isolates lacking class I ipiO variants are virulent on Rpi-blb1 potato. Mol. Plant Microbe Interact. **22:** 1535–1545.

Chaparro-Garcia, A., Wilkinson, R.C., Gimenez-Ibanez, S., Findlay, K., Coffey, M.D., Zipfel, C., Rathjen, J.P., Kamoun, S., and Schornack, S. (2011). The receptor-like kinase SERK3/BAK1 is required for basal resistance against the late blight pathogen *Phytophthora infestans* in *Nicotiana benthamiana*. PLoS ONE **6:** e16608.

Chen, Y., Liu, Z., and Halterman, D.A. (2012). Molecular determinants of resistance activation and suppression by *Phytophthora infestans* effector IPI-O. PLoS Pathog. **8:** e1002595.

Chisholm, S.T., Coaker, G., Day, B., and Staskawicz, B.J. (2006). Host-microbe interactions: Shaping the evolution of the plant immune response. Cell **124:** 803–814.

Chung, E.H., da Cunha, L., Wu, A.J., Gao, Z., Cherkis, K., Afzal, A.J., Mackey, D., and Dangl, J.L. (2011). Specific threonine phosphorylation of a host target by two unrelated type III effectors activates a host innate immune receptor in plants. Cell Host Microbe **9:** 125–136.

Collier, S.M., and Moffett, P. (2009). NB-LRRs work a "bait and switch" on pathogens. Trends Plant Sci. **14:** 521–529.

Deslandes, L., Olivier, J., Peeters, N., Feng, D.X., Khounlotham, M., Boucher, C., Somssich, I., Genin, S., and Marco, Y. (2003). Physical interaction between RRS1-R, a protein conferring resistance to bacterial wilt, and PopP2, a type III effector targeted to the plant nucleus. Proc. Natl. Acad. Sci. USA **100:** 8024–8029.

Dodds, P.N., Lawrence, G.J., Catanzariti, A.M., Teh, T., Wang, C.I., Ayliffe, M.A., Kobe, B., and Ellis, J.G. (2006). Direct protein interaction underlies gene-for-gene specificity and coevolution of the flax resistance genes and flax rust avirulence genes. Proc. Natl. Acad. Sci. USA **103:** 8888–8893.

Eitas, T.K., and Dangl, J.L. (2010). NB-LRR proteins: Pairs, pieces, perception, partners, and pathways. Curr. Opin. Plant Biol. **13:** 472–477.

Elmore, J.M., Lin, Z.J., and Coaker, G. (2011). Plant NB-LRR signaling: Upstreams and downstreams. Curr. Opin. Plant Biol. **14:** 365–371.

Fry, W.E., Gruenwald, N.J., Cooke, D.E.L., McLeod, A., Forbes, G.A., and Cao, K. (2008). Population genetics and population diversity of *Phytophthora infestans*. In Oomycete Genetics and Genomics, K. Lamour and S. Kamoun, eds (Hoboken, NJ: John Wiley & Sons), pp. 139–164.

Gilroy, E.M., et al. (2011). Presence/absence, differential expression and sequence polymorphisms between PiAVR2 and PiAVR2-like in *Phytophthora infestans* determine virulence on R2 plants. New Phytol. **191:** 763–776.

Gilroy, E.M., et al. (2007). Involvement of cathepsin B in the plant disease resistance hypersensitive response. Plant J. **52:** 1–13.

Haas, B.J., et al. (2009). Genome sequence and analysis of the Irish potato famine pathogen *Phytophthora infestans*. Nature **461:** 393–398.

Hein, I., Gilroy, E.M., Armstrong, M.R., and Birch, P.R. (2009). The zig-zag-zig in oomycete-plant interactions. Mol. Plant Pathol. **10:** 547–562.

Jia, Y., McAdams, S.A., Bryan, G.T., Hershey, H.P., and Valent, B. (2000). Direct interaction of resistance gene and avirulence gene products confers rice blast resistance. EMBO J. **19:** 4004–4014.

Jones, J.D., and Dangl, J.L. (2006). The plant immune system. Nature **444:** 323–329.

Karimi, M., Inzé, D., and Depicker, A. (2002). GATEWAY vectors for *Agrobacterium*-mediated plant transformation. Trends Plant Sci. **7:** 193–195.

Kim, T.W., Guan, S., Sun, Y., Deng, Z., Tang, W., Shang, J.X., Sun, Y., Burlingame, A.L., and Wang, Z.Y. (2009). Brassinosteroid signal transduction from cell-surface receptor kinases to nuclear transcription factors. Nat. Cell Biol. **11:** 1254–1260.

Krasileva, K.V., Dahlbeck, D., and Staskawicz, B.J. (2010). Activation of an *Arabidopsis* resistance protein is specified by the in planta association of its leucine-rich repeat domain with the cognate oomycete effector. Plant Cell **22:** 2444–2458.

Lindbo, J.A. (2007). TRBO: A high-efficiency tobacco mosaic virus RNA-based overexpression vector. Plant Physiol. **145:** 1232–1240.

Liu, J., Elmore, J.M., Lin, Z.J., and Coaker, G. (2011). A receptor-like cytoplasmic kinase phosphorylates the host target RIN4, leading to the activation of a plant innate immune receptor. Cell Host Microbe **9:** 137–146.

Lokossou, A.A., Park, T.H., van Arkel, G., Arens, M., Ruyter-Spira, C., Morales, J., Whisson, S.C., Birch, P.R., Visser, R.G., Jacobsen, E., and van der Vossen, E.A. (2009). Exploiting knowledge of *R/Avr* genes to rapidly clone a new LZ-NBS-LRR family of late blight resistance genes from potato linkage group IV. Mol. Plant Microbe Interact. **22:** 630–641.

Moffett, P., Farnham, G., Peart, J., and Baulcombe, D.C. (2002). Interaction between domains of a plant NBS-LRR protein in disease resistance-related cell death. EMBO J. **21:** 4511–4519.

Mora-García, S., Vert, G., Yin, Y., Caño-Delgado, A., Cheong, H., and Chory, J. (2004). Nuclear protein phosphatases with Kelch-repeat domains modulate the response to brassinosteroids in *Arabidopsis*. Genes Dev. **18:** 448–460.

Nakagawa, T., Kurose, T., Hino, T., Tanaka, K., Kawamukai, M., Niwa, Y., Toyooka, K., Matsuoka, K., Jinbo, T., and Kimura, T. (2007). Development of series of gateway binary vectors, pGWBs, for realizing efficient construction of fusion genes for plant transformation. J. Biosci. Bioeng. **104:** 34–41.

Oh, S.K., et al. (2009). *In planta* expression screens of *Phytophthora infestans* RXLR effectors reveal diverse phenotypes, including activation of the *Solanum bulbocastanum* disease resistance protein Rpi-blb2. Plant Cell **21:** 2928–2947.

Oliva, R., et al. (2010). Recent developments in effector biology of filamentous plant pathogens. Cell. Microbiol. **12:** 1015.

Panstruga, R., and Dodds, P.N. (2009). Terrific protein traffic: The mystery of effector protein delivery by filamentous plant pathogens. Science **324:** 748–750.

Peart, J.R., et al. (2002). Ubiquitin ligase-associated protein SGT1 is required for host and nonhost disease resistance in plants. Proc. Natl. Acad. Sci. USA **99:** 10865–10869.

Raffaele, S., et al. (2009). Remorin, a solanaceae protein resident in membrane rafts and plasmodesmata, impairs potato virus X movement. Plant Cell **21:** 1541–1555.

Rafiqi, M., Bernoux, M., Ellis, J.G., and Dodds, P.N. (2009). In the trenches of plant pathogen recognition: Role of NB-LRR proteins. Semin. Cell Dev. Biol. **20:** 1017–1024.

Ratcliff, F.G., MacFarlane, S.A., and Baulcombe, D.C. (1999). Gene silencing without DNA. rna-mediated cross-protection between viruses. Plant Cell **11:** 1207–1216.

Rooney, H.C., Van't Klooster, J.W., van der Hoorn, R.A., Joosten, M.H., Jones, J.D., and de Wit, P.J. (2005). *Cladosporium* Avr2 inhibits tomato Rcr3 protease required for Cf-2-dependent disease resistance. Science **308:** 1783–1786.

Shabab, M., Shindo, T., Gu, C., Kaschani, F., Pansuriya, T., Chintha, R., Harzen, A., Colby, T., Kamoun, S., and van der Hoorn, R.A. (2008). Fungal effector protein AVR2 targets diversifying defense-related cys proteases of tomato. Plant Cell **20:** 1169–1183.

Stassen, J.H., and Van den Ackerveken, G. (2011). How do oomycete effectors interfere with plant life? Curr. Opin. Plant Biol. **14:** 407–414.

van der Hoorn, R.A., and Kamoun, S. (2008). From guard to decoy: A new model for perception of plant pathogen effectors. Plant Cell **20:** 2009–2017.

van der Lee, T., Robold, A., Testa, A., van 't Klooster, J.W., and Govers, F. (2001). Mapping of avirulence genes in *Phytophthora infestans* with amplified fragment length polymorphism markers selected by bulked segregant analysis. Genetics **157:** 949–956.

Vleeshouwers, V.G., Raffaele, S., Vossen, J., Champouret, N., Oliva, R., Segretin, M.E., Rietman, H., Cano, L.M., Lokossou, A., Kessel, G., Pel, M.A., and Kamoun, S. (2011). Understanding and exploiting late blight resistance in the age of effectors. Annu. Rev. Phytopathol. **49:** 25.21–25.25.

Win, J., Kamoun, S., and Jones, A.M. (2011). Purification of effector-target protein complexes via transient expression in *Nicotiana benthamiana*. Methods Mol. Biol. **712:** 181–194.

Win, J., Morgan, W., Bos, J., Krasileva, K.V., Cano, L.M., Chaparro-Garcia, A., Ammar, R., Staskawicz, B.J., and Kamoun, S. (2007). Adaptive evolution has targeted the C-terminal domain of the RXLR effectors of plant pathogenic oomycetes. Plant Cell **19:** 2349–2369.
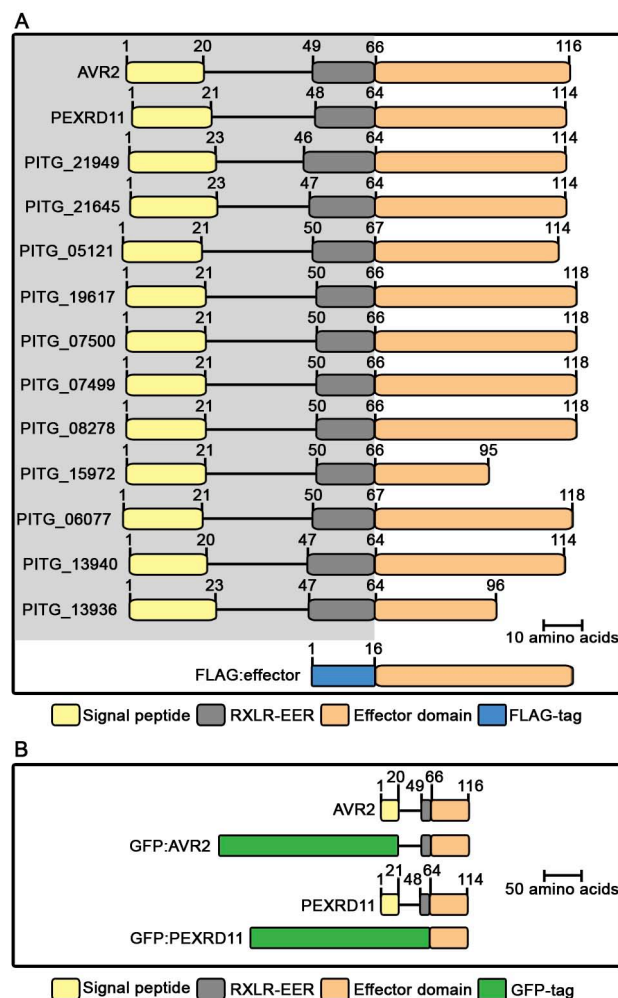
Supplemental Figure 1. Schematic representation of AVR2 family fusion constructs used in co-IPs. **(A)** The C-terminal effector domains (orange box) of twelve of the AVR2 family members were fused to the FLAG epitope tag at the N-terminus in place of the signal peptide and RXLR domain (highlighted in grey). For PEXRD11, the FLAG epitope tag was added in place of the signal peptide region alone. **(B)** The mature AVR2 protein (excluding the signal peptide region) and PEXRD11 effector domain were fused to the green fluorescent protein (GFP) at the N-terminus to create the fusion proteins GFP:AVR2 and GFP:PEXRD11, respectively. Numbers indicate position of the amino acid residues.
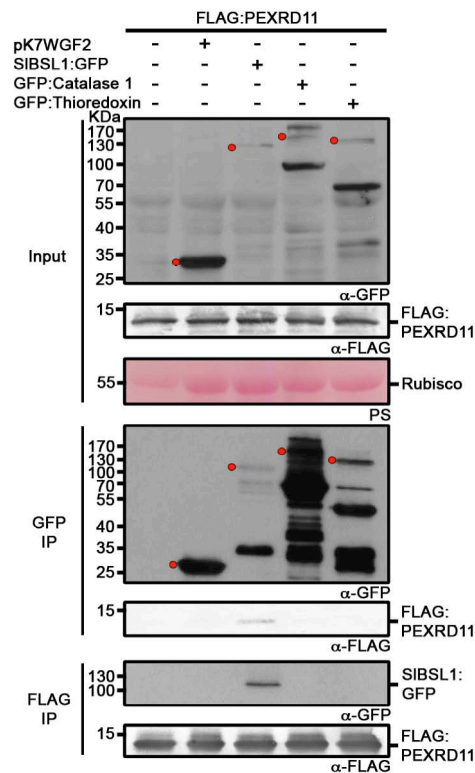
1

Supplemental Figure 2. Immunoblots showing that *P. infestans* PEXRD11 specifically associates with Sl-BSL1 *in planta*. FLAG:PEXRD11 was transiently expressed alone, with pK7WGF2 or with GFP-tagged putative target proteins in *N. benthamiana*. Immunoprecipitates obtained with anti-FLAG or anti-GFP antiserum and total protein extracts were immunoblotted with appropriate antisera. The expected sizes of the GFP fusion proteins are indicated by red dots in the crude extracts and GFP co-IP probed with anti-GFP antibody. PS, Ponceau stain.
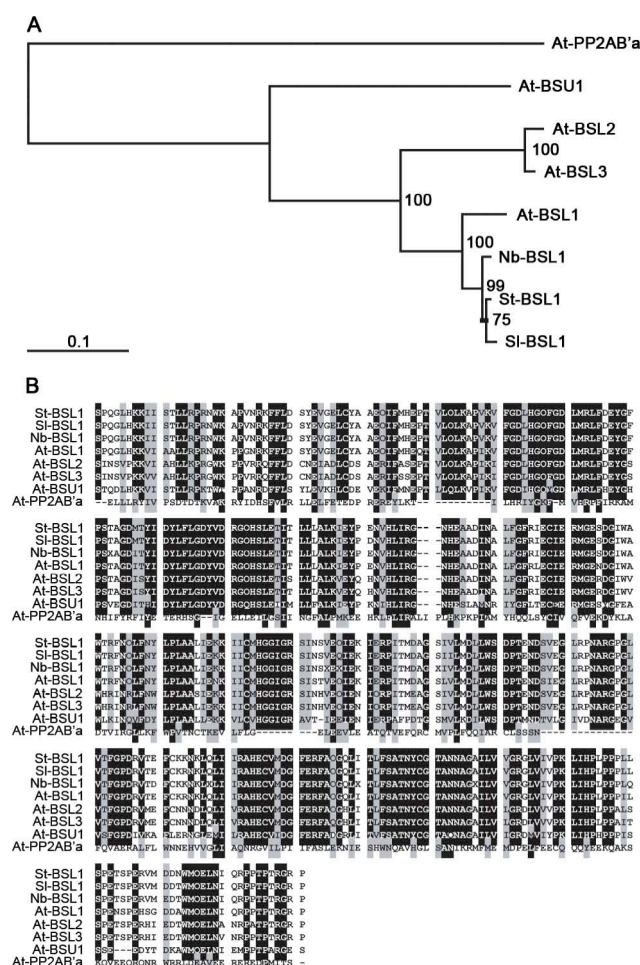
Supplemental Figure 3. Sequence analysis confirms that BSL1 from *Solanum tubersosum* (potato), *Solanum lycopersicum* (tomato) and *Nicotiana benthamiana* are orthologs of *A. thaliana* BSL1. **(A)** Phylogenetic analysis reveals that from the *Arabidopsis* BSU family, At-BSL1 is the closest ortholog of the potato, tomato and *N. benthamiana* BSL1 amino acid sequences. TOPALi v2.5 (Milne et al. 2009) was used to draw a Neighbour joining tree with a 500 bootstrap, midpoint rooted, with sequences of the C-terminal phosphatase domains of each protein **(B)**. The tree was re-rooted in FigTree v1.3.1 (http://tree.bio.ed.ac.uk/software/figtree/) to the outlier AtPP2AB'a (At3g09880). AtPP2AB'a (At3g09880), which is a component of the brassinosteroid pathway (Tang et al., 2011) was included as an outlier as the BSL phosphatases are members of the PP2A family. The tree was visualized using treeview (http://taxonomy.zoology.gla.ac.uk/rod/treeview.html). **(B)** Sequence alignment of *Arabidopsis* BSU family and potato, *N. benthamiana* and tomato BSL1 phosphatase domain-containing regions used for the Neighbour joining tree in **(A)**. Sequences were aligned using ClustalW from 522 to 869 amino acids for the BSL1 proteins, 658 to 1005 amino acids for At-BSL2, 647 to 994 for At-BSL3, 467 to 810 for At-BSU1 and 185 to 495 amino acids for At-PP2AB'a proteins. The graphic view was generated in BioEdit and imported into TOPALi v2.5 for phylogenetic analysis.
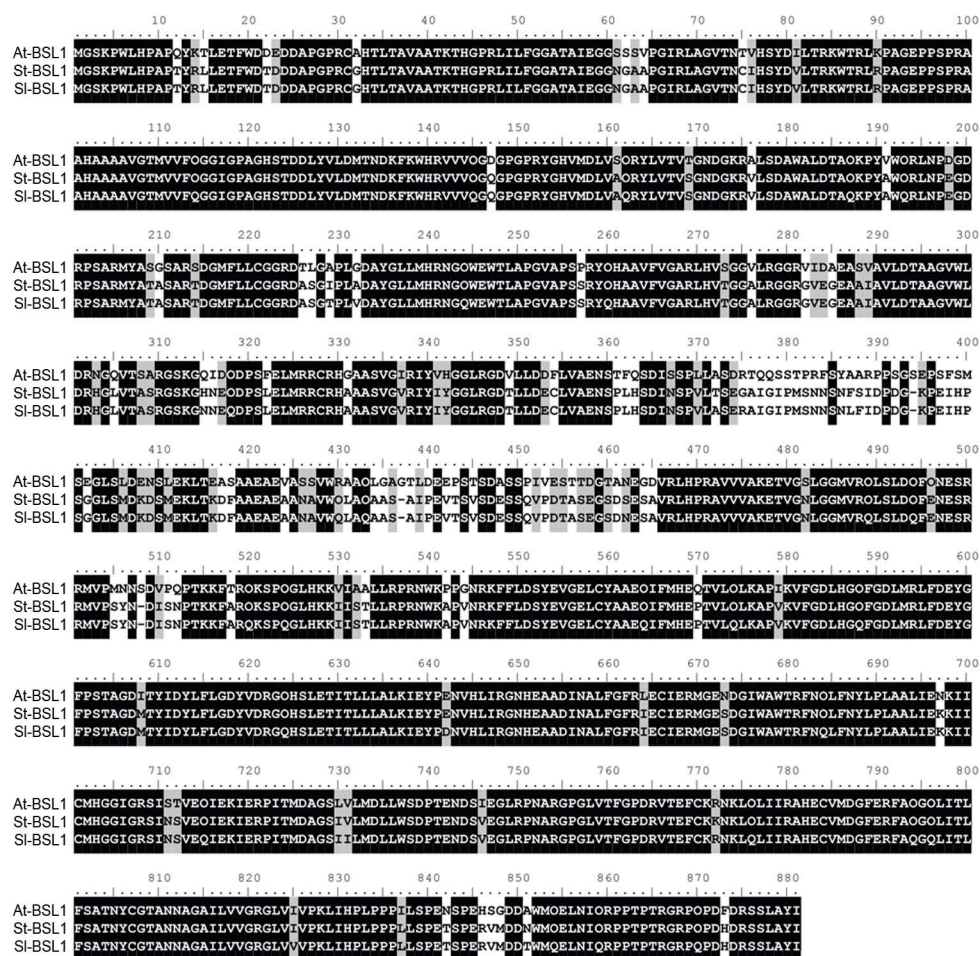
Supplemental Figure 4. *Arabidopsis, Solanum tubersosum* (potato) and *Solanum lycopersicum* (tomato) BSL1 full-length amino acid sequences are highly conserved. Sequences were aligned using ClustalW and the graphic view generated in BioEdit. The N-terminal kelch-repeat domain covers amino acids 18-369 and the phosphatase domain is from 520-869 amino acids.
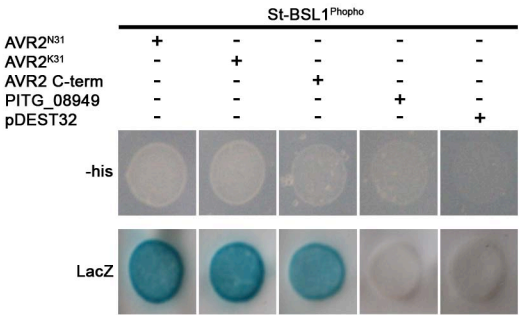
Supplemental Figure 5. Y2H analysis illustrating that *P. infestans* AVR2^{K31}, AVR2^{N31} and the C-terminal effector domain of AVR2 (amino acids 66-116) interact with the phosphatase domain (amino acids 520-881) of potato BSL1 (St-BSL1) *in vivo*. Both LacZ (giving blue colour) and His3 (providing growth on medium lacking histidine [-his]) reporter genes were activated. Empty vector (pDEST32) and the effector PITG_08949 (Gilroy et al., 2011) were used as negative controls.
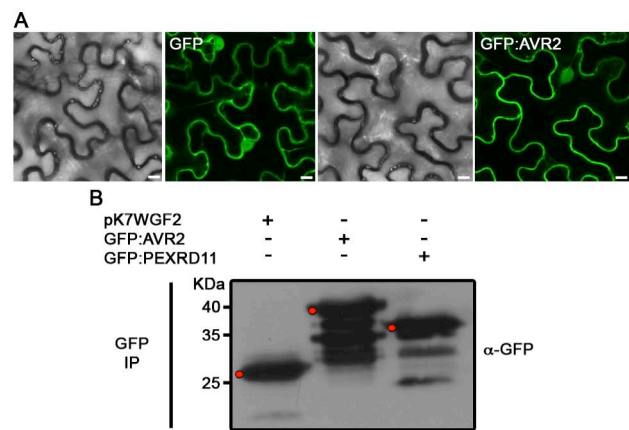
Supplemental Figure 6. Localization and stability of *P. infestans* AVR2 *in planta*. **(A)** GFP:AVR2 localizes at the cell periphery and weakly in the cytoplasm and nucleus. **(B)** GFP:AVR2 and GFP:PEXRD11 fusion proteins were partially cleaved when expressed *in planta*. pK7WGF2, GFP:AVR2 and GFP:PEXRD11 were transiently expressed in *N. benthamiana*. Immunoprecipitates obtained with anti-GFP antiserum were immunoblotted with appropriate antisera. The expected sizes of the GFP fusion proteins are indicated by red dots. Scale bars represent 10 µm.
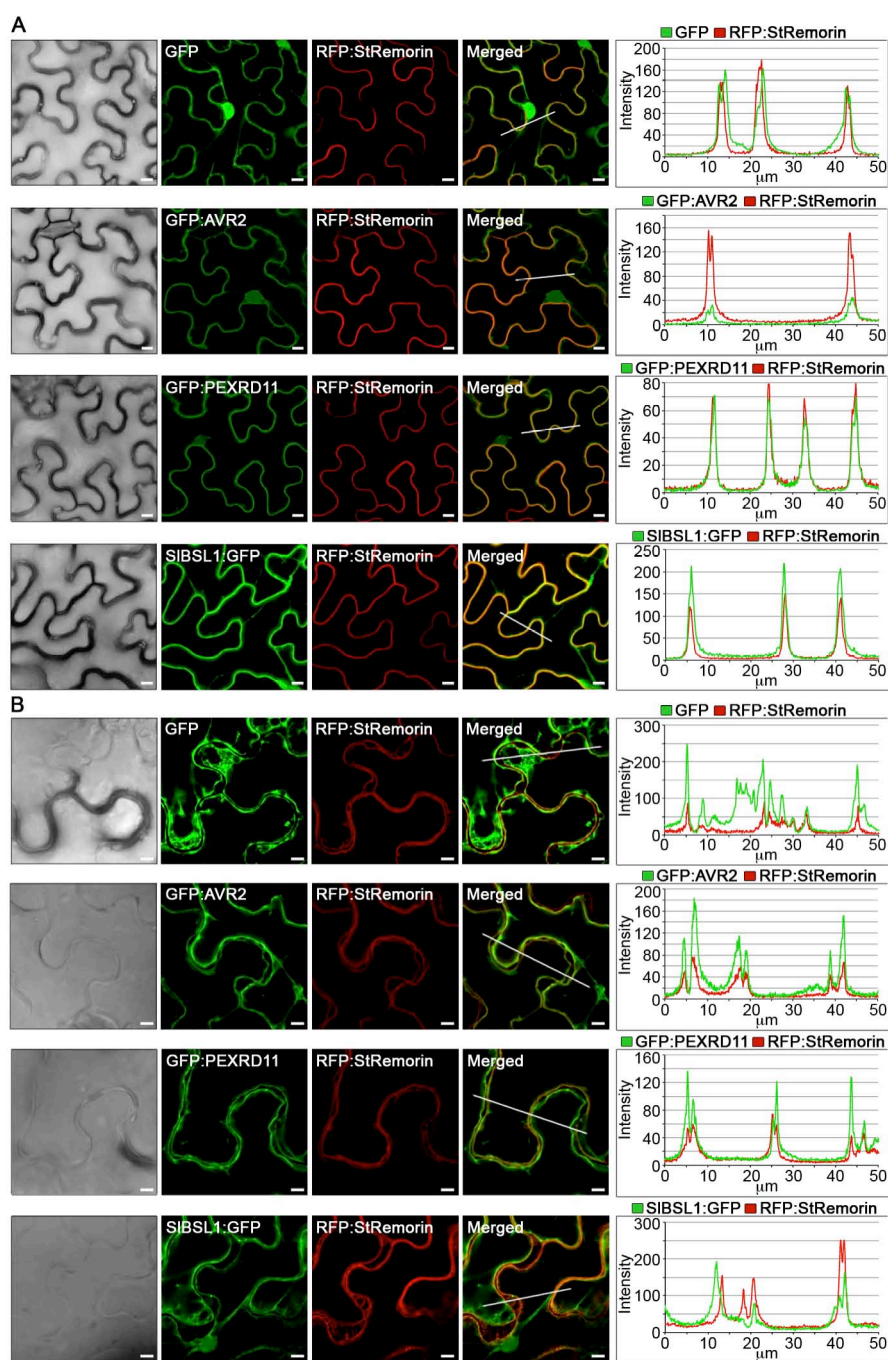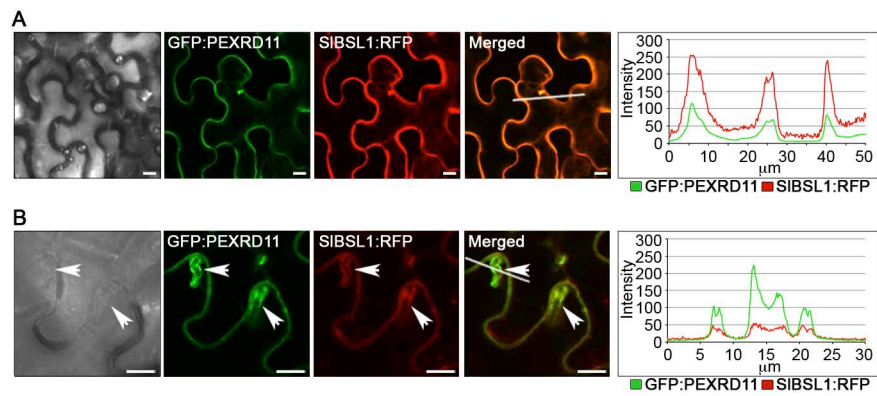
Supplemental Figure 7. *P. infestans* AVR2 and PEXRD11 co-localize with the plasma membrane-associated protein Remorin *in planta*. **(A)** GFP:AVR2, GFP:PEXRD11 and, to a large extent, SlBSL1:GFP co-localized with RFP:StRemorin at the plasma membrane when co-expressed transiently in *N. benthamiana*. **(B)** Following salt-induced plasmolysis, GFP:AVR2 and GFP:PEXRD11 clearly co-localized with RFP:StRemorin, as illustrated by overlapping peaks in the fluorescence intensity graphs. However, SlBSL1:GFP only partially co-localized with RFP:StRemorin following salt-induced plasmolysis. Pictures taken 3 dpi, scale bars represent 10 **(A)** or 5 **(B)** μm.
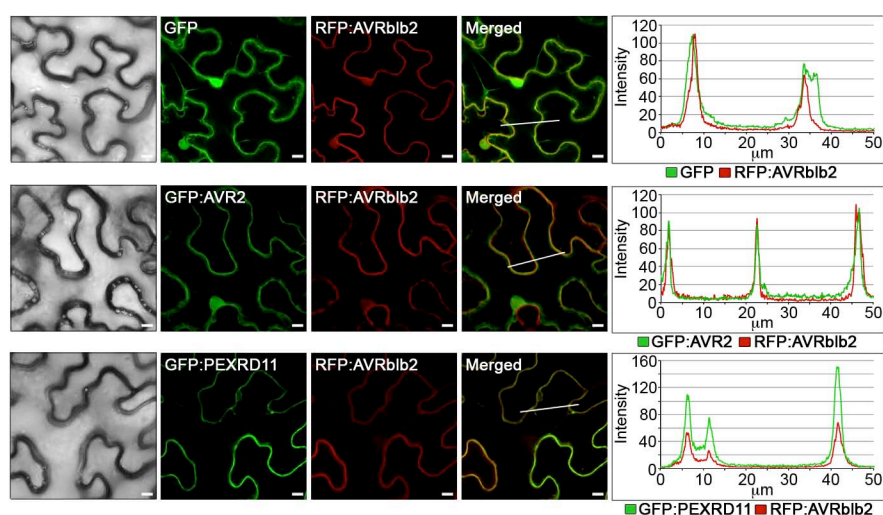
Supplemental Figure 8. *P. infestans* AVR2 and PEXRD11 co-localize with the *P. infestans* plasma membrane-associated effector AVRblb2 in planta. GFP:AVR2 and GFP:PEXRD11 co-localized with RFP:AVRblb2 in *N. benthamiana*, as illustrated by overlapping peaks in the fluorescence intensity graphs. Pictures taken 4 dpi, scale bars represent 10 μm.
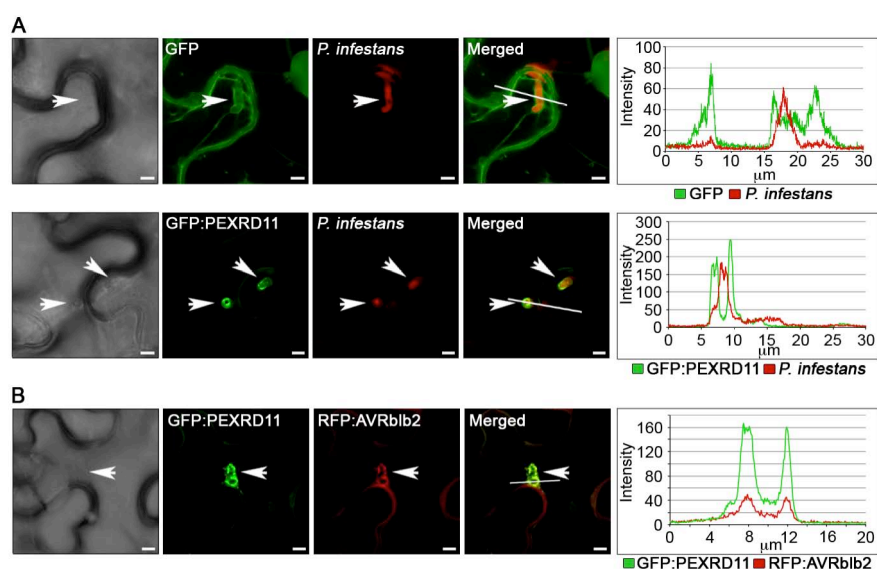
Supplemental Figure 9. *P. infestans* PEXRD11 accumulates around haustoria and co-localizes with the perihaustorial-localized effector AVRblb2 *in planta*. **(A)** *P. infestans* (red) infected *N. benthamiana* cells preferentially accumulated GFP:PEXRD11 (green) around haustoria (arrowheads), when compared to the expression of GFP alone, which maintained high levels of fluorescence throughout the cell. **(B)** *P. infestans* infected cells accumulated GFP:PEXRD11 and RFP:AVRblb2 preferentially at sites of haustorial penetration (arrowheads). Pictures were taken at 4 dpi, scale bars represent 5 μm.

Supplemental Figure 10. Tomato BSL1 and *P. infestans* PEXRD11 colocalize *in planta* and accumulate around haustoria. **(A)** Transient expression of GFP:PEXRD11 and SlBSL1:RFP fusion proteins revealed similar patterns of localization for the two markers, accumulating at the cell periphery and within the cytoplasm. **(B)** *P. infestans* infected cells accumulated GFP:PEXRD11 and SlBSL1:RFP at sites of haustorial penetration (arrowheads). Scale bars represent 10 µm.
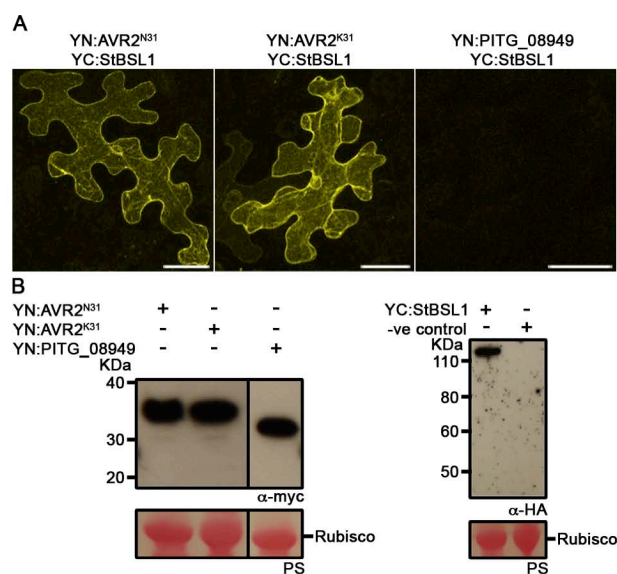
Supplemental Figure 11. AVR2 is in close proximity to St-BSL1 at the cell periphery and within the cytosol. **(A)** Bimolecular fluorescence complementation (BiFC) illustrated an association between YN:AVR2[N31] or YN:AVR2[K31] and YC:StBSL1 at the plasma membrane (smooth cell surface fluorescence) and in the cytosol, but not within nuclei. The N-terminus (YN) of YFP was fused to full length AVR2[N31], AVR2[K31], or PITG_08949 (excluding the signal peptide region) and co-expressed with St-BSL1 fused to the C-terminal half of YFP (YC). Images are projected stacks of 50 confocal images covering a depth of 43 μm. Scale bars represent 50 μm. **(B)** Immunoblots showing that YN:AVR2, YN:PITG_08949 and YC:StBSL1 fusion proteins were stable *in planta*. Immunoblots were probed with GFP antisera. PS, Ponceau stain.
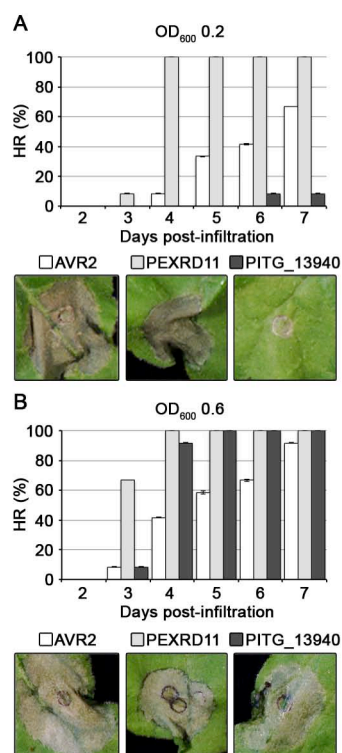
Supplemental Figure 12. PITG_13940 activates R2-mediated hypersensitivity (HR). AVR2, PEXRD11 or PITG_13940 were co-expressed with R2 in *N. benthamiana* using agroinfiltration and a final OD_{600} of 0.2 **(A)** or 0.6 **(B)**. HR (%) indicates the percentage of infiltration sites showing a confluent zone of cell death. Error bars represent +/- SE. Graphs represent 2 biological replicates, of 6 inoculation sites for each combination. Pictures were taken 4 days post-infiltration.
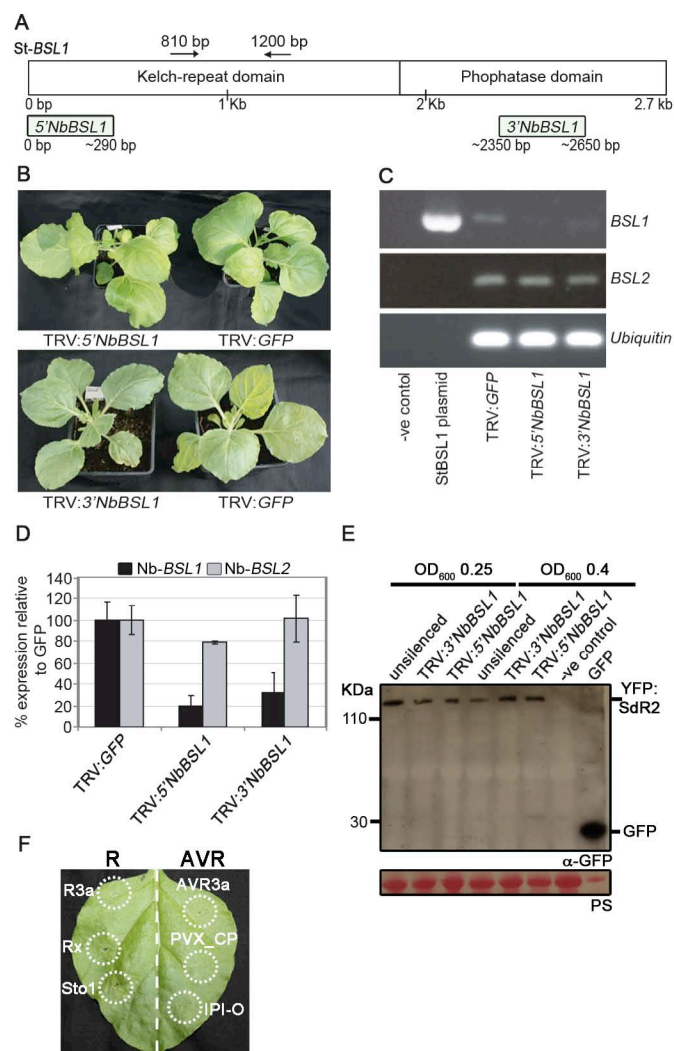
Supplemental Figure 13. Virus-induced gene silencing (VIGS) of *BSL1* in *N. benthamiana*. **(A)** Schematic representation of St-*BSL1*, which was used as a reference to design the locations of fragments of Nb-*BSL1* that were cloned into the TRV-based silencing construct (green boxes). Arrows indicate the locations of primer-annealing sites for amplification of a fragment of Nb-*BSL1* used to confirm silencing by RT-PCR. **(B)** *BSL1*-silenced plants did not show any marked phenotypic alterations when compared to TRV:*GFP* control plants. Using semi-quantitative **(C)** and quantitative **(D)** RT-PCR, VIGS of Nb-*BSL1* with either 3' or 5' silencing constructs resulted in a specific reduction in expression of Nb-*BSL1* in *N. benthamiana* compared to the expression of a second *BSU*-like gene, Nb-*BSL2*. **(E)** Immunoblots showing that R2 is stable in the *BSL1* VIGS plants. Total protein extracts were immunoblotted with an anti-GFP antibody. PS, Ponceau stain. **(F)** Expression of either effectors (AVR3a, PVX-CP, ipiO1) or corresponding resistance proteins (R3a, Rx, Sto1) alone in *BSL1*-silenced plants did not induce cell death.

13
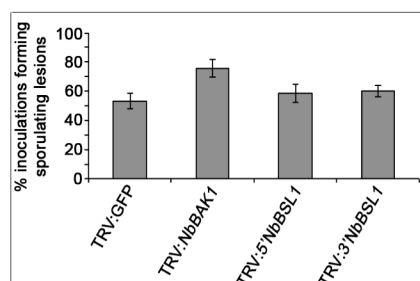
Supplemental Figure 14. VIGS of *BSL1* in *N. benthamiana* did not affect colonisation by *P. infestans*. Percentage of inoculation sites showing sporulation 6 days post-inoculation on plants expressing TRV:*GFP*, TRV:*NbBAK1*, TRV:*5'NbBSL1* or TRV:*3'NbBSL1*. There was no statistically significant increase in susceptibility to *P. infestans* for plants expressing TRV:*GFP*, TRV:*5'NbBSL1* or TRV:*3'NbBSL1*, when compared to *BAK1*-silenced plants which display increased susceptibility to *P. infestans* (Chaparro-Garcia *et al.*, 2011). Statistical analysis was performed using the Holm-Sidak method in a one-way ANOVA on the Sigmaplot statistical software package. *P. infestans* colonisation was significantly different only on TRV:*NbBAK1* plants. The graph represents 7 biological replicates, each using 4 plants for each construct, 3 leaves inoculated per plant (84 inoculation sites per construct).
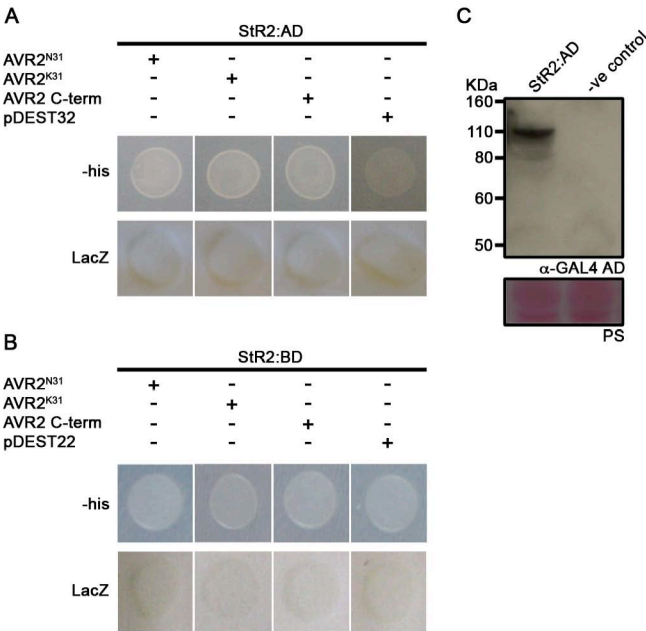
Supplemental Figure 15. Y2H analysis failed to demonstrate a direct inter-action between AVR2 and R2. **(A, B)** Y2H analysis illustrating that AVR2^{K31}, AVR2^{N31}, and the C-terminal effector domain of AVR2 (amino acids 66-116) do not interact with potato R2 in vivo. Both LacZ (giving blue colour) and His3 (providing growth on synthetic-complete (-leu, -trp) medium lacking histidine [-his]) reporter genes were not activated. Empty vector (pDEST32 or pDEST22 as indicated) was used as a negative control. AVR2 and R2 were fused to both the activation and binding domains of α-GAL4 **(B)** Immunoblots showing that St-R2 was stable when expressed in yeast cells. Total protein extracts were immunoblotted with an antibody that targets the GAL4 activation domain (α-GAL4 AD). PS, Ponceau stain.

Supplemental Table 1. Plant proteins that specifically associated with AVR2 family effectors after co-immunoprecipitation as identified by mass spectrometry. Eight AVR2 homologs formed protein complexes detectable by LC-MS/MS.

Annotation for plant proteins identified in association with effector*	GenBank Accession number	Number of unique peptides matched to plant proteins in each effector co-immunoprecipitation experiment†								
		FLAG: RFP	PITG_ 21645	PITG_ 13940	PEX RD11	PITG_ 07500	PITG_ 07499	PITG_ 08278	PITG_ 06077	PITG_ 21949
Catalase 1	JQ886090	0	4	2	3	3	5	3	1	4
Serine/threonine-protein phosphatase BSL1 (BSU1-like protein 1)	JQ886089	0	7	0	8	0	0	0	0	0
Thioredoxin peroxidase	JQ886091	0	2	4	2	5	4	2	3	0

*Annotations were part of the sequences downloaded from source

†Peptide spectrum matching results were from Mascot (Matrix Science) searches and only those matching with probability score >95% are shown; Numbers reflect the number of unique peptides matched per protein; FLAG:RFP was used as negative control. Matching peptide sequences and other detail information are reported in Table S2.

Supplemental Table 2. Details of primers used in this study.

Primer name	Sequence (5'>3')
5AVR2	CACCATGCTGCATGCAGCTCCAGGTGCCAAG
3AVR2	TTAACTCCTCTTGTCACCCTTAATTTTCAAATG
5RD11	CACCACCGGAGGCTTACTGGATAAGA
3RD11	CTATTTGTACCCCTGTCCCTTTG
5BSL1	CACCATGGGTTCAAAGCCATGGC
3BSL1	AATATAGGCAAGTGAGCTCCGG
5Cat1	CACCGATCCATACAAGTATCGTCCGTCA
3Cat1	TCATATGCTTGGTCTCACATTAAG
5Thper	CACCGCTTGCTCTGCTTCTTCTACA
3Thper	TCATATGGATGCAAAGTATTC
3BSL1_kel	TGATTTCTGCCTTGCGAAC
5BSL1_phos	CACCATGCCTCAAGGATTGCATAAAAAGATC
FStrem13	AAAAAGCAGGCTTCATGGCAGAATTGGAAGCT
RStrem13	AGAAAGCTGGGTCTCAAAATATTCCAAGGAT
5Nterm_R2	CACC GCTGATGCCTTTCTATCATTTG
3Nterm_R2	TCACAACATATAATTCCGCTTCAAC
5StBSL1-1	AAAGCAGGCTTCATGGGTTCAAAGCCATGG
3StBSL1-1	GAAAGCTGGGTATTAAATATAGGCAAGTGAGCT
5StBSL1-2	GGGGACAAGTTTGTACAAAAAAGCAGGCT
3StBSL1-2	GGGGACCACTTTGTACAAGAAAGCTGGG
5StBSL-CT	AAAGCAGGCTTCATGGTGAGGCAATTGTCA
5BSL1-290	TAAAGAATTCATGGGTTCAAAGCCAT
3BSL1-290	TTTTGTTAACTCACCGGCAGGTCTAAGT
5BSL1-300	ATTTGAATTCTGCATTGAGAGAATCCCACA
3BSL1-300	TTTAGTTAACACGATCAGGCCCAAATGTTA
5BSL1-RT	AGGCGATAGACCGTCAGCTA
3BSL1-RT	CGCATAAGCTCCAAAGAAGG
5BSL2-RT	TGCACGCAGTTATGGAGAAG
3BSL2-RT	AACCAGCAGAATTCCCTTCA

Supplemental References:

Chaparro-Garcia, A., Wilkinson, R.C., Gimenez-Ibanez, S., Findlay, K., Coffey, M.D., Zipfel, C., Rathjen, J.P., Kamoun, S., and Schornack, S. (2011). The receptor-like kinase SERK3/BAK1 is required for basal resistance against the late blight pathogen phytophthora infestans in Nicotiana benthamiana. PLoS One **6,** e16608.

Gilroy, E.M., Breen, S., Whisson, S.C., Squires, J., Hein, I., Kaczmarek, M., Turnbull, D., Boevink, P.C., Lokossou, A., Cano, L.M., et al. (2011). Presence/absence, differential expression and sequence polymorphisms between PiAVR2 and PiAVR2-like in *Phytophthora infestans* determine virulence on R2 plants. New Phytol **191,** 10.1111/j.1469-8137.2011.03736.x.

Milne, I., Lindner, D., Bayer, M., Husmeier, D., McGuire, G., Marshall, D.F., and Wright, F. (2009). TOPALi v2: a rich graphical interface for evolutionary analyses of multiple alignments on HPC clusters and multi-core desktops. Bioinformatics **25,** 126-127.

Tang, W., Yuan, M., Wang, R., Yang, Y., Wang, C., Oses-Prieto, J.A., Kim, T.W., Zhou, H.W., Deng, Z., Gampala, S.S., et al. (2011). PP2A activates brassinosteroid-responsive gene expression and plant growth by dephosphorylating BZR1. Nature cell biology **13,** 124-131.

Host Protein BSL1 Associates with *Phytophthora infestans* RXLR Effector AVR2 and the *Solanum demissum* Immune Receptor R2 to Mediate Disease Resistance

Diane G.O. Saunders, Susan Breen, Joe Win, Sebastian Schornack, Ingo Hein, Tolga O. Bozkurt, Nicolas Champouret, Vivianne G.A.A. Vleeshouwers, Paul R.J. Birch, Eleanor M. Gilroy and Sophien Kamoun

This information is current as of August 10, 2012

Supplemental Data	**http://www.plantcell.org/content/suppl/2012/08/02/tpc.112.099861.DC1.html**
Permissions	https://www.copyright.com/ccc/openurl.do?sid=pd_hw1532298X&issn=1532298X&WT.mc_id=pd_hw1532298X
eTOCs	Sign up for eTOCs at: http://www.plantcell.org/cgi/alerts/ctmain
CiteTrack Alerts	Sign up for CiteTrack Alerts at: http://www.plantcell.org/cgi/alerts/ctmain
Subscription Information	Subscription Information for *The Plant Cell* and *Plant Physiology* is available at: http://www.aspb.org/publications/subscriptions.cfm